Genomics, Proteomics & Bioinformatics , 2022, 1–26
doi: DOI HERE
Advance Access Publication Date: Day Month Year
Paper

Integrating Host-Pathogen Genomics to Enhance Wheat Resistance Against Septoria tritici Blotch

Alejandro Dominguez-Rondón,[1,*] Andrea Sánchez-Vallet[1] and Julio Isidro y Sánchez [1,*]

[1]Centro de Biotecnologia y Genómica de Plantas (CBGP, UPM-INIA) Universidad Politécnica de Madrid (UPM) - Instituto Nacional de Investigación y Tecnologia Agraria y Alimentaria (INIA) Campus de Montegancedo-UPM 28223-Pozuelo de Alarcón, (Madrid), Spain

*Corresponding author. alejandro.dominguez@upm.es, j.isidro@upm.es

FOR PUBLISHER ONLY Received on Date Month Year; revised on Date Month Year; accepted on Date Month Year

Abstract

Septoria tritici blotch, caused by *Zymoseptoria tritici*, is a major disease that reduces wheat yields worldwide. Disease severity depends on interactions between wheat resistance genes and fungal virulence factors, including effectors and pathogenicity-related proteins. In this study, we integrated host and pathogen genomic data to improve resistance breeding. By combining greenhouse experiments with genome-wide association studies, we identified quantitative trait loci associated with resistance on wheat chromosomes 1A and 4B, linked to receptor-like kinases, glycosyltransferases, and transcription factors. In *Z. tritici*, we detected candidate virulence genes, including a potential effector (*ZtIPO323_000490*), a histone acetyltransferase (*ZtIPO323_088990*), and a polyketide synthase (*ZtIPO323_124400*), suggesting roles for epigenetic regulation and secondary metabolites in pathogenicity. We also applied genomic selection models incorporating host-pathogen interactions to predict disease outcomes. While integrating pathogen data improved prediction accuracy in some cases, strong isolate × cultivar specificity complicated modeling, highlighting the need for targeted breeding strategies. Overall, this study identifies key genetic factors influencing wheat resistance and *Z. tritici* virulence. The identified genes and quantitative trait loci provide valuable targets for breeding programs, supporting the development of resistant wheat varieties and contributing to more sustainable disease management in wheat production.

Key words: Genomic Selection, GWAS, wheat, Septoria Tritici Blotch, host-pathogen interaction

Introduction

Septoria tritici blotch (STB), caused by the ascomycete *Zymoseptoria tritici*, is the third most significant disease affecting wheat (Savary et al., 2019). It reduces global wheat production by an estimated 2.5% annually, with losses in untreated, susceptible cultivars reaching up to 50% (Fones and Gurr, 2015).

The primary control method for STB is synthetic fungicides. However, their widespread use disrupting ecosystem balance, increases production costs, and accelerates resistance development (Torriani et al., 2015; Cheval et al., 2017). Te dynamic adaptation of the pathogen is driven by its rapid sexual reproduction cycle (Feurtey et al., 2023), highlighting the need for sustainable management strategies. A promising alternative is resistance breeding, which aims to develop wheat varieties with enhanced genetic resistance (Brown et al., 2015). Genetic resistance can be qualitative or quantitative. Qualitative resistance is controlled by *Stb* genes, with 23 *Stb* major resistant genes identified to date (Brown et al., 2015). These genes follow a gene-for-gene model, where a plant resistance gene recognizes a pathogen avirulence factor, conferring isolate-specific resistance.

In contrast, quantitative resistance is largely additive, governed by oligogenic or polygenic systems with small-to-moderate effects (Brown et al., 2015). It provides broad-spectrum resistance independent of specific pathogen isolates. Over 150 Quantitative Trait Loci (QTL) and 190 marker-trait associations (MTA) have been reported in QTL mapping and association mapping studies (Ando et al., 2018; Kollers et al., 2013; Vagndorf et al., 2017; Gerard et al., 2017; Muqaddasi et al., 2019; Gurung et al., 2014; Mekonnen et al., 2021; Yates et al., 2019; Louriki et al., 2021; Yang et al., 2022; Thauvin et al., 2024). However, few genome-wide association studies (GWAS) have focused on the pathogen (Sánchez-Vallet et al., 2017; Bartoli and Roux, 2017; Amezrou et al., 2023, 2024), leaving its genetic basis largely unknown. Only three avirulence genes (Avr3D1, Avrstb6, and Avrstb9) have been

fully characterized (Zhong et al., 2017; Kema et al., 2018; Meile et al., 2018; Amezrou et al., 2023). Identifying fungal pathogenicity sources and their interactions with wheat resistance is crucial for developing durable resistance strategies and reducing reliance on fungicides (Torriani et al., 2015).

Genomic Selection (GS) offers a promising approach for improving complex traits like disease resistance by estimating genomic breeding values (GEBV) (Meuwissen et al., 2001), reducing both time and costs (Isidro et al., 2016). Bernardo (2014) proposed a model integrating GWAS with GS, leveraging significant GWAS hits to enhance predictions. This approach has improved wheat and STB resistance in wheat compared to conventional GS methods (Spindel et al., 2016; Odilbekov et al., 2019; Alemu et al., 2021; Zakieh et al., 2023). Furthermore, recent studies have demonstrated the potential of integrating dual-genome prediction models to capture both host and pathogen genomic contributions in Fusarium head blight resistance (Hudson et al., 2024). However, no such approach has been applied to *Z.tritici* despite its economic importance and complex host-pathogen interactions.

This study aims to improve wheat resistance to STB by i) identifying novel QTL associated with STB in wheat and *Z. tritici* populations, ii) enhancing genomic prediction accuracy for host resistance, and iii) assessing the potential for predicting the pathogenicity of future *Z.tritici* strains. While previous studies have focused primarily on either the host or the pathogen, we hypothesize that integrating fungal genomic data will provide deeper insights into the genetic basis of quantitative resistance and improve selection accuracy. To test this, we conducted GWAS on both host and pathogen populations and applied a Host-Pathogen Genomic Integration Model on a wheat population exposed to genetically diverse fungal isolates.

Methods

Plant and Fungal Material

Phenotypic Data

ANDREA

Genotypic Data

Wheat genotyping was conducted by the North Central Small Grains Genotyping Laboratory at USDA-ARS-ETSARC in Fargo, ND, using the Illumina 90k single nucleotide polymorphism (SNP) array chip Wang et al. (2014). Variants were filtered based on Minor Allele Frequency (MAF) (MAF < 0.05) and missingness per variant (missingness $< 20\%$), resulting in a final dataset of approximately 21K SNPs.

The fungal genome was sequenced via Whole-Genome Sequencing (WGS), with 1 GB of raw data requested per sample. A total of 119 strains were analyzed following Genome Analysis Toolkit (GATK) guidelines (Geraldine A. Van der Auwera, 2020). Paired-end reads were trimmed using Trimmomatic v0.39 (Bolger et al., 2014) and mapped to the reference genome IPO323 (Goodwin et al., 2011) using the mem algorithm from BWA v0.7.14 with default options (Li and Durbin, 2009). Duplicate reads were tagged using Samtools v0.1.19 (Li et al., 2009), MarkDuplicatesSpark, and BaseQualityRecalibrator. Variants were called per sample using GATK's HaplotypeCaller (ploidy set to 1), retaining only biallelic markers. Markers with MAF < 0.05 or $>20\%$ missing data were excluded. Given the high variability of fungal accessory chromosomes, only core chromosome (CC 1–13) markers were considered. The final dataset of 665K markers was annotated using SnpEff (Cingolani et al., 2012).

We computed Linkage Disequilibrium (LD) R^2 between all pairs of markers within 20 kb windows per region using PLINK (Purcell et al., 2007), and modelled the decay of R^2 over distance using a non-linear model as described by Hill and Weir (1988). The filtered marker data were also used to generate additive Genomic Relationship Matrices (GRMs) for inclusion in mixed models, following the VanRaden method. GRMs for each fungal mix were calculated from the corresponding marker matrices, using the mean marker values of the strains in each mix.

Genome-Wide Association Studies

Wheat analyses were conducted separately for each treatment using a two-step approach. First, we estimated wheat genotype Best Linear Unbiased Estimators (BLUEs) using the following model:

$$y = l + m + r + \epsilon \tag{1}$$

where y represents the vector of phenotypes, l, m, and r denote wheat genotypes, mixes, and replication fixed effects, and ϵ is the residual error. The BLUES per wheat line was used as the response variable in the second step.

We applied two multi-locus models available in the Genome Association and Prediction Integrated Tool (GAPIT) (Lipka et al., 2012) to identify Marker-Trait Associations (MTAs): Bayesian-information and linkage disequilibrium iteratively nested keyway (BLINK) (Huang et al., 2018) and Fixed and Random Model Circulating Probability Unification (FarmCPU) (Liu et al., 2016). To control population structure and minimize false positives, we incorporated Principal Components (PCs) and a kinship matrix (K). We assessed model performance under the null hypothesis using Quantile-Quantile (Q-Q) plots of observed versus expected -log10(p) values. The Bonferroni-corrected significance threshold was set at $-log10(0.05/n)$, where $n = 20969$, resulting in a threshold of 5.6. Manhattan plots, illustrated with `CMplot` (Yin et al., 2021), showed the distribution of significant markers across chromosomes. Additionally, we identified genes within a 50 kb region around each significant marker and annotated their secreted protein functions and associated Gene Ontology (GO) terms using the Uniprot database (Bateman et al., 2024). If no gene was found inside the window, we retrieved the information of the closest gene to the MTA.

We conducted the pathogen GWAS independently for each cultivar using the isolates BLUPs. Markers with a Logarithm of the Odds (LOD) score greater than 7.8 were considered significant. We calculated pairwise LD between all marker pairs within a 20 kb window using PLINK (Purcell et al., 2007). Candidate genes were identified within a 4 kb window for each MTA, from the latest annotation available (Lapalu et al., 2023). Finally, we visualized selected regions using the `LDheatmap` package (Shin et al., 2006).

Functional Annotation and Gene Expression Analysis

We predicted N-terminal secretion signals using the Hidden Markov Model (HMM) scoring method in SignalP 6.0 (Teufel et al., 2022) and identified transmembrane domains with DeepTMHMM 1.0 (Hallgren et al., 2022). Effector probabilities were assessed with EffectorP 3.0 (Sperschneider and Dodds, 2022), while conserved protein domains were detected using InterProScan

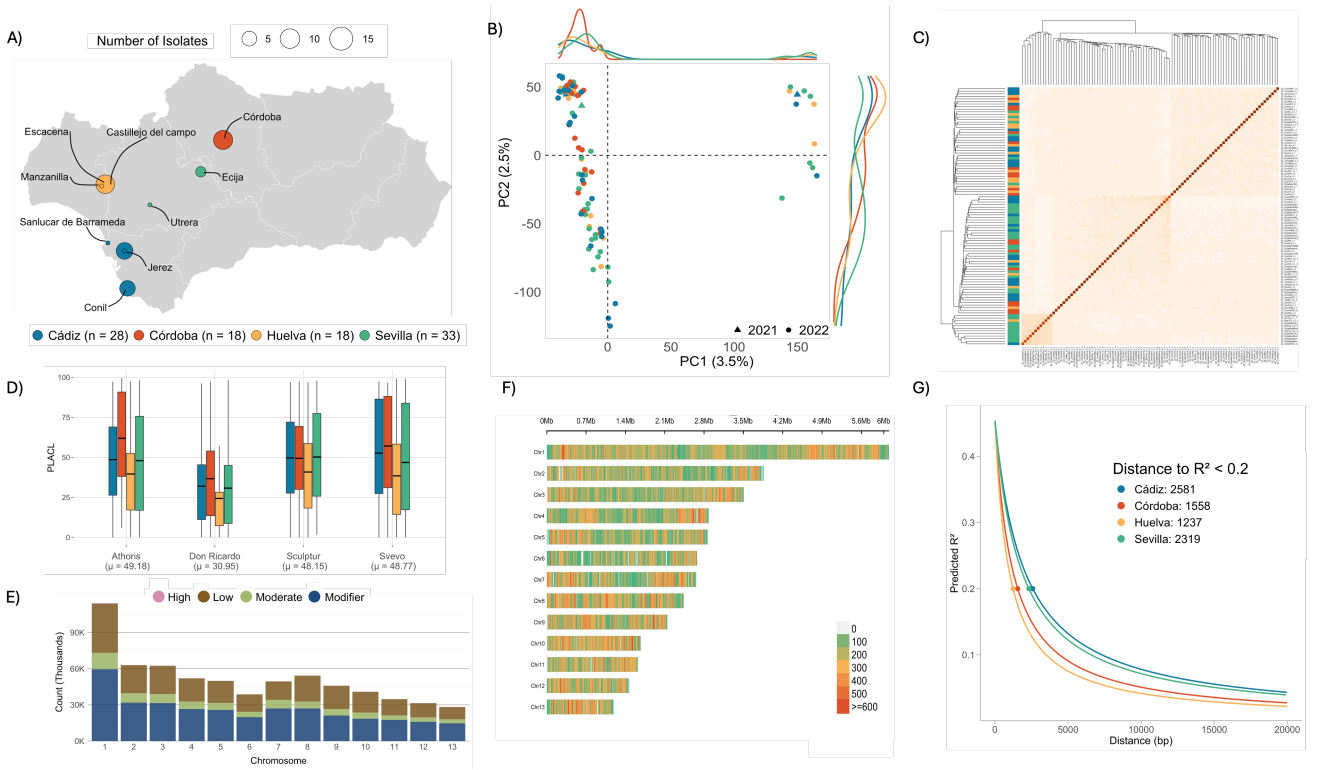

Fig. 1: ***Zymoseptoria tritici* population genotypic and phenotypic information**. (A) Location and number of isolates sampled from regions in Andalucía (Cádiz, Córdoba, Huelva, and Sevilla). (B) Principal Component Analysis (PCA) representation. (C) Heatmap of the isolates' Genomic Relationship Matrix. (D) Phenotypic distribution of Percentage of Leaf Area by Lesion (PLACL) per region. (E) Predicted markers' putative impact. (F) Marker density per chromosome, computed in 10 kb bins. (G) Linkage Disequilibrium (LD) decay per region.

(Blum et al., 2024), applying HMM searches against the PFAM 37.0 database (Mistry et al., 2020). Protein descriptions were assigned based on BLASTp searches against protein databases from all organisms.

RNA-seq data from in-planta samples were obtained from a previous study (Lapalu et al., 2023), covering time points at 4, 11, 13, and 20 days post-inoculation (dpi). We computed gene expression quantified as transcripts per million (TPM) counts. We inferred pairwise log2-fold expression change for in-planta RNAseq samples compared to the glucose culture medium. Genes with a $log2|FC| > 2$ were considered differentially expressed during the infection.

Wheat Genomic Selection

We implemented a five-fold cross-validation (CV) by randomly partitioning wheat lines into Training (TRS) and Validation sets (VS). First, we estimated BLUES for each plant:strain combination by solving Equation 2 using the `lmer` function in the `lme4` package (Bates et al., 2015):

$$y = plant : strain + s + t + r + \epsilon \quad (2)$$

where y represents the phenotype vector (PLACL), $plant : strain$, s, t and r denotes the plant:strain combination, set, trial and replicate fixed effects, and ϵ the residuals. Next, we implemented the second-stage model using the Bayesian Genomic Best Linear Unbiased Predictions (BGLR) package (Pérez and de los Campos, 2014), applying the following mixed model equation:

$$y = X\beta + Z_1 u_1 + Z_2 u_2 + \epsilon \quad (3)$$

where y is the concatenated vector of BLUEs from Equation 2, X represents the design matrix for fixed effects, β the vector of fixed effects, Z_1 and Z_2 the design matrices for the random effects of wheat lines and septoria mixes, u_1 and u_2 the vectors of specific genetic values for wheat lines and septoria mixes, and ϵ the vector of residual errors.

In addition, we designed models accounting for wheat-fungi interactions and weighted adjustment models. To prevent overfitting, GWAS was performed only in the TRS at each iteration, with significant markers introduced as fixed effects. If no SNP surpassed the Bonferroni threshold, the one with the lowest p-value was selected. If one to three SNPs exceeded the threshold, all were included; if more than three did, only the top three were retained. Selected markers were then removed from the marker matrix before recalculating the Genomic Relationship Matrix (GRM).

We tested four different covariance structures to solve Equation 3, using either the Genomic Relationship (G) or the Identity matrix (I) for wheat lines (w) and fungi mixes (m). Consequently, we tested four modeling approaches (Standard, Standard+interaction, Weighted, and Weighted+interaction) across 30 CV rounds, with four matrix combinations (I_w/I_m,

I_w/G_m, G_w/I_m, G_w/G_m). We assessed model performance by computing prediction accuracy, defined as the Pearson correlation coefficient between BLUEs from Equation 2 and BLUPs from Equation 3.

Additionally, we estimated genetic parameters and analyzed variance distribution across 16 models. We quantified the variance explained by each effect as the ratio of estimated genetic variation to total variation, determining the proportional contribution of the host, mixes, host-mix interactions, and errors in each model.

Zymoseptoria tritici Genomic Prediction

We ran 500 iterations of 5-fold CV within the TRS population and analyzed each host separately to ensure consistent model evaluation across iterations. We modeled all traits using a single-stage approach, applying the mixed model equation:

$$y = i + t + yr + brep + r + \epsilon \quad (4)$$

where i is the random effect of the isolates, and $i, t, yr, brep$ and r are trial, year, biological replicates, and region fixed effects, and e is the error. Prediction accuracy was calculated as the correlation between BLUPs and the BLUEs corresponding to the tested cultivar. Then we computed the mean and standard deviation for each region across iterations.

Results

Z. tritici and Wheat Population

The regions and number of isolates extracted are shown in Figure 1. A Principal Component Analysis revealed minimal population structure, with the first two principal components accounting for approximately 6% of the variance (1.B). Although a subset of 12 samples segregated along PC1 (Figure S3.C), no clustering was observed based on year or region.

Disease symptoms and sporulation varied by host-isolate combination (Figure 1.D). Isolates from Córdoba isolates exhibited the highest average PLACL values, followed by those from Cádiz and Sevilla, while Huelva isolates were the least virulent. In addition, Córdoba strains exhibited higher pycnidia per leaf and lesion in three out of four cultivars (Figure S2.

Marker classification revealed that more than half of the variants had a modifier impact, while approximately 0.25% (1,736) were predicted to have a high impact (Figure 1.E, Table S2). Marker density ranged from one SNP every 41 base pairs on chromosome 10 to one every 61 base pairs on chromosome 2 (Figure 1.F, Table S1). On average, a variant was detected every 53 bp, suggesting that MTA precision could approach single-gene resolution, given the average gene spacing in *Z. tritici* (1,080 bp). Genome-wide LD decay (Figure 1.G) also varied by isolate origin, with strains from Cádiz exhibiting the longest LD decay (∼2.5 kb), whereas those from Huelva showed significantly shorter decay distances.

Wheat PCA (Figure 2.A) revealed that the first two PCs explained approximately 25% of the variance, indicating genetic differentiation among subpopulations. Cultivars and lines exhibited greater genetic similarity compared to landraces.

Wheat genome-wide association study

In total, we identified 7 MTAs. Mix 1 and Mix 2 yielded 4 and 2 hits associated with pycnidia production, while a single hit linked to PLACL was found for Mix 3. No significant markers were detected for Mix 4. The MTAs were located on chromosomes 1B, 1D, 2B, 2D, 4A, and 6B (Figure 2.B). Notably, none of the markers overlapped across treatments, suggesting a lack of broad-spectrum resistance (Table 1).

High-confidence candidate genes are summarized in Supplementary Table S3. The nearest genes to markers on chromosome 1D encode two isoforms of a protein kinase and three proteins containing DUF295, UBX, and DUF4283 domains. Close to the marker on chromosome 3D, we identified three genes encoding a glycosyltransferase, a zinc finger protein, and a TF-B3 domain-containing protein. The closest genes to markers *D_contig01739_117*, *Tdurum_contig13746_167*, *Excalibur_c3683_328*, and *Kukri_c31681_147* were located approximately 0.5, 0.09, 0.5, and 0.2 Mb away, respectively. These genes encode an AP2/ERF domain-containing protein, an RRM domain-containing protein, adenylyl-sulfate kinase, and an aldehyde oxygenase.

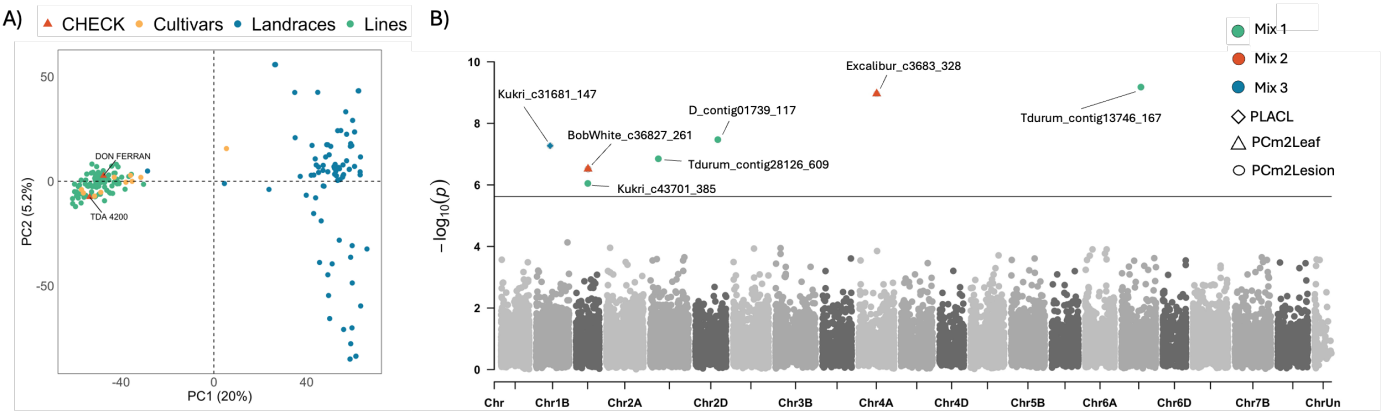

Fig. 2: **Population structure and Genome-Wide Association Study (GWAS) results for the wheat population.** (A) Principal Component Analysis (PCA) of the wheat population. (B) Manhattan plot displaying marker positions on the x-axis and their $-log(p\text{-}value)$ on the y-axis. The horizontal black line represents the Bonferroni significance threshold at 5.6.

Septoria genome-wide association study

We identified 13 significant markers through cultivar-specific GWAS (Table S4). Most markers were identified in Don Ricardo (n = 8), followed by Svevo and Sculptur (n = 2 each), with a single hit in Athoris. No markers overlapped between cultivars. In Don Ricardo strains, significant hits were associated with all three traits, whereas in other cultivars, markers were linked only to pycnidia-related traits. The MTAs were distributed across chromosomes 1 ($n = 5$), 3, 4, 8 ($n = 3$), 9, 11, and 13. Marker *X11_849459* was the only MTA linked to multiple traits, influencing both PCm2Leaf and Lesion, with p-values of 2.8×10^{-10} and 4.56×10^{-13}, the latter representing the most significant association detected. None of the identified markers were located in regions previously associated with avirulence genes.

We identified 29 candidate genes near the MTAs. Only one gene, *ZtIPO323_003820*, overlapped with more than one hit, suggesting distinct mechanisms underlying conidial production and lesion severity.

Six out of the 29 genes showed no (TPM = 0) or very low expression (TPM < 5) across all infection stages. In contrast, 5 genes exhibited differential expression ($log2|FC| > 2$) compared to the control medium. These genes encoded a histone acetyltransferase, a mono-functional catalase, a polyketide synthase, a major facilitator superfamily protein, and an uncharacterized protein. The latter gene encodes a small secreted protein (258 amino acids) enriched with seven cysteine residues in strong LD with multiple variants spanning a 3.3 kb region (chr1:236139-239403). While two additional genes were located in this region, only *ZtIPO323_000490* was predicted to be secreted and serve as a putative effector.

Allelic variation (Figure 4.B) clearly distinguished between more and less pathogenic strains. *ZtIPO323_000490* was downregulated during early infection stages, reaching peak expression at 13 dpi, marking the onset of the necrotic phase (Figure 4.C). Additionally, this protein showed no homology with other fungal species. Collectively, these findings strongly suggest that *ZtIPO323_000490* functions as a fungal effector.

Host-Pathogen Genomic Integration Prediction Model

The covariance structure was the main factor driving prediction accuracy, as shown in Figure 5. Models using G_w/G_m and G_w/I_m achieved the highest accuracy, whereas I_w/G_m and I_w/I_m models consistently performed around 0. Although modeling the response with both GRMs ($G_w/_m$) did not significantly outperform other approaches, it consistently provided better predictions than models relying solely on wheat genomic data. This effect was most pronounced when accounting for host-mix interactions, except for Mix 4. Despite these improvements, prediction accuracy remained highly dependent on the treatment being predicted. In some cases, the difference between the best and worst-performing mixes exceeded 0.1, though the ranking varied across approaches. The mix also influenced prediction variability. For instance, Mix 2 exhibited the highest variability, while Mix 4 had the lowest, despite both originating from the same region and having similar pathogenic levels. Incorporating host-pathogen interactions improved prediction accuracy in both Standard and Weighted approaches, with the largest increase observed in Mix 4 (from 0.19 to 0.28). However, weighted models failed to enhance prediction accuracy and decreased it across all treatments. This decline was likely due to the limited number of significant markers detected in the GWAS performed on TRS subsets during cross-validation (Figure S10). Additionally, the strong impact of covariance structure seen in the first two approaches was absent here, as all four combinations yielded similar results.

Model variance estimations

Table 2 summarizes the parameter estimates. In the first approach, host heritability (H^2) was higher in models using I_w, while mix heritability (M^2) increased significantly when the mix marker-based GRM (G_w) was applied. Regardless of the matrix used, adding the interaction term in the Standard approach reduced both H^2 and M^2. Consequently, the host-pathogen interaction (HM^2) accounted for a larger proportion of the variability than the combined effects of the host and pathogen in three out of four models. Moreover, HM^2 varied substantially with the variance-covariance structure, ranging from 6% in the G_w/I_m scenario to 54% in the I_w/G_m model.

In the Weighted approach, host heritability H^2 remained consistent across all four models but explained less variance than in the previous strategy, suggesting a smaller role for wheat genetic effects. This aligns with the lower prediction accuracies observed in these models. Mix heritability M^2 increased again in models using G_w instead of I_w, exceeding 1.7%. In models incorporating both GWAS hits and interaction effects, host and pathogen heritability decreased further, falling below 10% and 1%, respectively. The variance attributed to interaction effects remained stable, except in the I_w/G_m model, where it dropped significantly to 29%.

Z.tritici Genomic Predictions

Within-region prediction accuracies varied substantially depending on the cultivar (Figure 6). For instance, predictions for Svevo consistently produced the highest accuracies, while those for Don

Mix	Trait	SNP	Chr	Pos	P-value	MAF	Effect
Mix 1	PCm2Leaf	Kukri_c43701_385	Chr1D	251994101	8.95×10^{-7}	0.0619	10.70
		Tdurum_contig28126_609	Chr2B	173072036	1.42×10^{-7}	0.4149	-9.46
		D_contig01739_117	Chr2D	476750339	3.38×10^{-8}	0.2088	6.40
		Tdurum_contig13746_167	Chr6B	412780966	6.64×10^{-10}	0.4021	-11.61
Mix 2	PCm2Lesion	BobWhite_c36827_261	Chr1D	256969209	3.03×10^{-7}	0.0735	32.04
		Excalibur_c3683_328	Chr4A	386229406	1.09×10^{-9}	0.0838	25.73
Mix 3	PLACL	Kukri_c31681_147	Chr1B	298435348	5.34×10^{-8}	0.0773	16.19

Table 1. Significant associations identified in the GWAS of the wheat population.

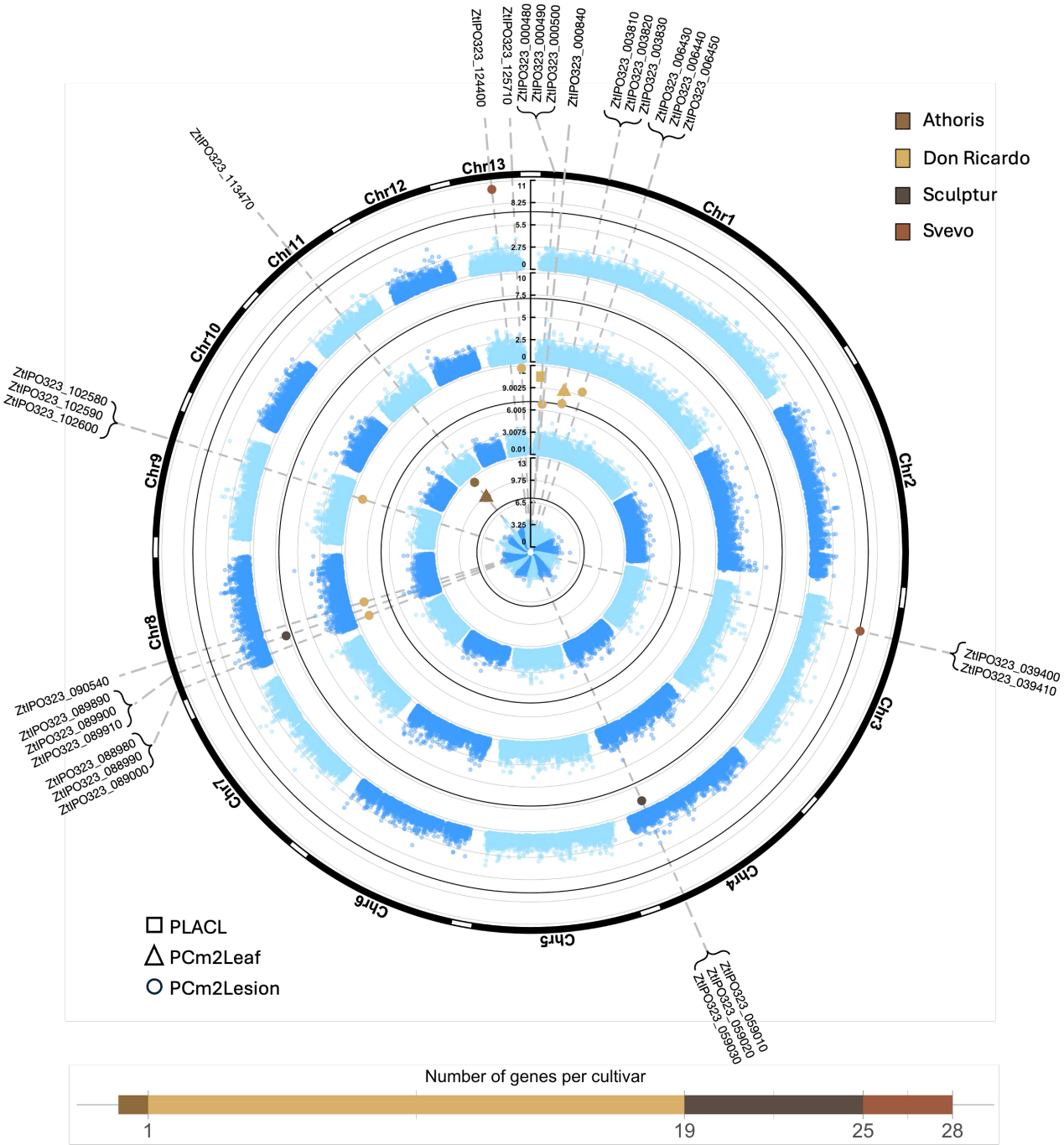

Fig. 3: **Cultivar Specific Genome Wide Association Studies Results**. Circular Manhattan showing marker position and $-log(p\text{-}value)$ on the X and Y-axis. The horizontal black line represents the Bonferroni significance threshold (7.1). Each ring corresponds to the results of a specific cultivar, ranging from Athoris (inner ring) to Svevo (outer ring). Colors indicate significant markers identified in each cultivar, and shapes denote the trait significantly associated with the marker. Candidate genes located within a 4 kb window of the significant markers are also shown.

Ricardo were the lowest. Although significant differences were observed among regions, these differences were highly cultivar-dependent, thus no single region was consistently better predicted across all cultivars. Moreover, the three traits were predicted with similar accuracy, but the prediction patterns for each region differed, even within the same cultivar.

Overall, prediction reliability remained low throughout the analysis, with negative predictions resulting from high standard deviations. Huelva consistently exhibited the greatest variability

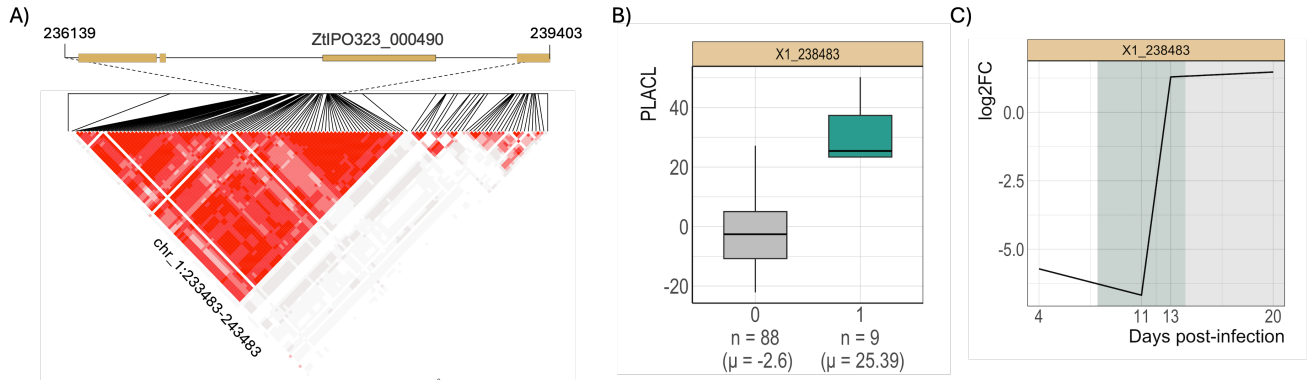

Fig. 4: ***ZtIPO323_000490*, a putative effector-like small secreted protein implicated in the quantitative pathogenicity of *Z. tritici***. A) Linkage disequilibrium (LD) plot depicting the correlation (r^2) between all pairs of markers within the region chr1:236139-239403. B) Allele differences for the MTA *X1_238483*. C) Log2-fold expression changes of *ZtIPO323_000490 in planta* vs control media (Glucose).

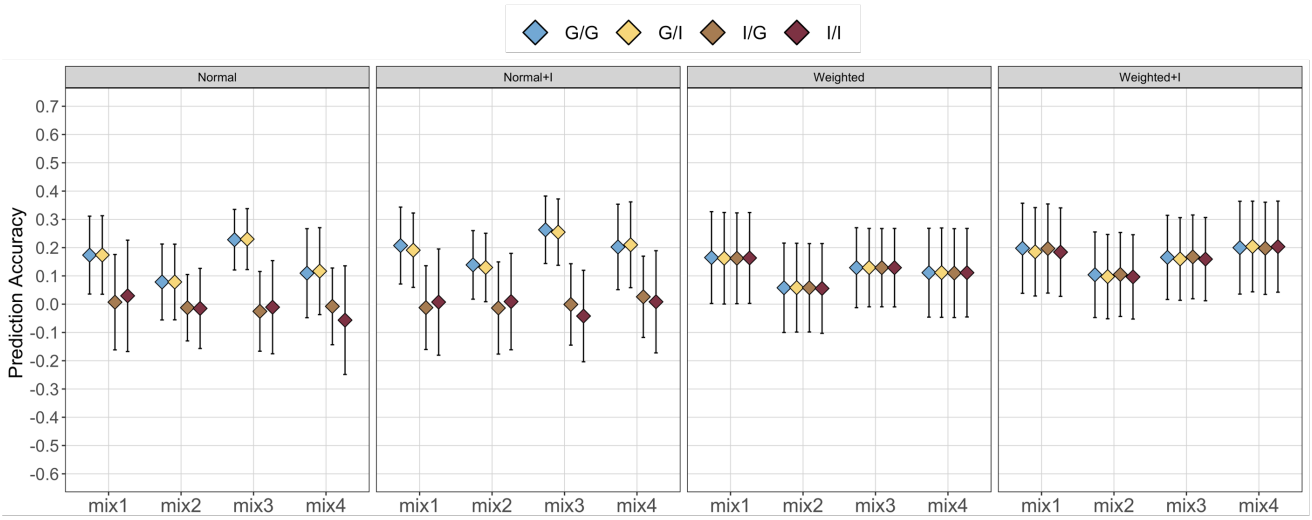

Fig. 5: **Prediction accuracy for dual-genome prediction models**.The notation G_w/G_m, G_w/I_m, I_w/G_m, and I_w/I_m denotes the kernel used for wheat (w) and *Z.tritici* mixes (m, where G represents the Genomic Relationship Matrix and I the identity matrix.

across all traits and cultivars, whereas Córdoba strains displayed the least. These discrepancies likely stem from the composition of the training set. Córdoba, containing the highest number of isolates (37 out of 119), had a greater likelihood of being represented in the TRS set, potentially leading to improved predictions compared to Huelva, which had fewer strains and a lower probability of inclusion. However, despite its larger representation, Córdoba still ranked among the lowest-performing regions in several scenarios.

Discussion

Wheat and Septoria Genome Wide Association Studies

We infected 200 lines of wheat with four fungal mixes. GWAS identified hits in three mixes, each containing three strains, but detected none in the mix containing a single isolate. This may be due to the limited impact of 22_*CorVal_L1* on resistance-associated regions or the varied host responses that obscured detection. Additionally, using a single isolate in Mix 4 may have reduced detection power, whereas incorporating multiple strains with similar virulence could enhance the signal.

The seven MTAs associated with adult-stage resistance spanned across 6 chromosomes. Two markers overlapped with previously reported QTL or MTAs from earlier studies. The marker on chromosome 2*B* colocalized with *QStb.ihar-2B.4*, identified by Piaskowska et al. (2021), and linked to necrosis and pycnidia coverage. Similarly, marker *Tdurum_contig13746_167* overlapped with *QStb.teagasc-6B.3*, mapped to chromosome 6*B* between 199 Mb and 529 Mb (Riaz et al., 2020). Another marker, *D_contig01739_117*, was located (14 Mb) to *QSTB12*, a QTL reported by Mekonnen et al. (2021) associated with the Septoria progress coefficient. Although none of the MTAs directly overlapped with known STB resistance genes, this does not indicate that the selected lines lack these genes, as their activation depends on the presence of the corresponding Avr proteins in the isolates, and vice versa, as previously noted. Moreover, we

Approach	Matrix	H^2	M^2	HM^2	Error Variance (%)
Standard	G_w/G_m	14.51 ± 1.73%	1.77 ± 0.34%	0 ± 0%	83.72 ± 1.82%
	G_w/I_m	14.66 ± 1.73%	0.27 ± 0.06%	0 ± 0%	85.07 ± 1.74%
	I_w/G_m	19.06 ± 1.87%	1.74 ± 0.38%	0 ± 0%	79.20 ± 1.98%
	I_w/I_m	19.22 ± 1.89%	0.27 ± 0.06%	0 ± 0%	80.51 ± 1.90%
Standard+I	G_w/G_m	11.41 ± 1.17%	0.79 ± 0.11%	28.86 ± 1.95%	58.95 ± 2.20%
	G_w/I_m	13.58 ± 1.66%	0.17 ± 0.03%	6.45 ± 0.61%	79.80 ± 1.59%
	I_w/G_m	10.50 ± 0.94%	0.53 ± 0.09%	54.55 ± 2.96%	34.42 ± 2.60%
	I_w/I_m	15.21 ± 1.60%	0.17 ± 0.04%	19.26 ± 1.41%	65.36 ± 2.01%
Weighted	G_w/G_m	10.73 ± 1.95%	1.82 ± 0.36%	0 ± 0%	87.44 ± 2.02%
	G_w/I_m	10.87 ± 1.92%	0.28 ± 0.06%	0 ± 0%	88.85 ± 1.93%
	I_w/G_m	10.71 ± 1.96%	1.83 ± 0.38%	0 ± 0%	87.46 ± 2.01%
	I_w/I_m	10.82 ± 1.89%	0.28 ± 0.06%	0 ± 0%	88.90 ± 1.89%
Weighted+I	G_w/G_m	8.62 ± 1.51%	0.82 ± 0.13%	29.60 ± 1.84%	60.96 ± 2.13%
	G_w/I_m	9.72 ± 1.99%	0.18 ± 0.03%	6.77 ± 0.73%	83.33 ± 2.04%
	I_w/G_m	8.60 ± 1.49%	0.81 ± 0.12%	29.66 ± 2.17%	60.93 ± 2.37%
	I_w/I_m	9.72 ± 1.95%	0.18 ± 0.03%	6.79 ± 0.68%	83.32 ± 2.04%

Table 2. Estimated genetic parameters. The table shows the percentage of variance explained by genetic components corresponding to the host (H^2), the mixes (M^2), and the host-mix interaction (HM^2), along with the percentage of total variance attributed to errors. Values represent the mean ± standard deviation. The notation G_w/G_m, G_w/I_m, I_w/G_m, and I_w/I_m denotes the kernel used for wheat (w) and *Z. tritici* mixes (m), where G represents the Genomic Relationship Matrix and I the identity matrix.

identified two MTAs near the genomic region mapped to *Stb10*. Specifically, markers associated with pycnidia per leaf and lesion surface were located 22 Mb and 27 Mb downstream of the designated *Stb10* QTL, which spans from 36 Mb to 230 Mb (Chartrain et al., 2005). The remaining two MTAs, located on chromosomes $1A$ and $4B$, have not been previously reported and may represent novel QTL linked to adult-stage resistance to STB in wheat.

Several genes within these QTL regions encode proteins or domains linked to resistance. For instance, kinase domains were identified in genes near markers *Kukri_c43701_385* on chromosome 1D and *Excalibur_c3683_328* on chromosome 4A. Since all three known *Stb* resistance genes,*Stb6*, *Stb16q*, and *Stb15*—encode receptor-like kinases (RLKs) (Saintenac et al., 2018, 2021; Hafeez et al., 2023), these candidate genes may also play a role in recognizing *Z. tritici* avirulence proteins. Additionally, a gene on chromosome $6B$ encodes a Glycosyltransferases, a protein family involved in biotic stress responses in wheat (He et al., 2018) and other plant-pathogen interactions, such as *Sclerotinia sclerotiorum* and *Botrytis cinerea* in rapeseed (Zhang et al., 2015). Other identified genes encode transcription factors, including zinc finger and B3 domains. Zinc finger proteins regulate responses to biotic and abiotic stress (Li et al., 2013), while the B3 transcription factor superfamily has been linked to plant stress responses (Wang et al., 2024) and an increased abundance of small secreted proteins in wheat (Sun et al., 2017). These candidate genes provide promising targets for further research.

On the pathogen side, we identified 29 candidate genes, six of which were differentially expressed throughout the infection. Among them, only one exhibited effector-like characteristics, while the remaining five likely play indirect roles in infection. The effector-like protein encodes a 250-amino acid peptide containing seven cysteine residues. Although its overall expression is lower than that of known effectors *AvrStb6* and *AvrStb9*, its differential expression relative to control media is comparable or even higher (see Supplementary Table S6). Further functional validation is required to determine its role in STB infection.

We also identified proteins involved in stress response, toxic compound degradation, and nutrient uptake. For instance, *ZtIPO323_006440* encodes a monofunctional catalase that degrades H_2O_2, a compound plants release to induce cellular damage and regulate responses (Hansberg et al., 2012). However, previous studies suggest that this catalase has little effect on modulating host-derived H_2O_2, and mutants lacking similar enzymes exhibit reduced spore germination (Mirzadi Gohari et al., 2024). This aligns with findings in *Neurospora crassa*, where the homologous Cat2 promotes asexual spore formation (Hansberg et al., 2012). Since the protein's peak expression coincides with pycnidia formation and its low H_2O_2-degrading activity, we hypothesize that its primary function is enhancing pycnidia production rather than detoxification.

We identified a fungal-specific histone acetyltransferase, Rtt109-like, belonging to the lysine acetyltransferase (KAT) family. KATs acetylate histone lysine residues, influencing chromatin remodeling, modulating DNA accessibility, and regulating gene expression (Rothbart and Strahl, 2014). Effector genes, often located in heterochromatic regions, require chromatin modifications for activation during host colonization (Freitag, 2017). Consequently, histone acetylation plays a crucial role in the spatiotemporal regulation of effector gene expression. Recently, Suarez-Fernandez et al. (2023) investigated the role of several KATs in *Z. tritici* growth, development, and virulence. Their study demonstrated that histone acetylation at effector loci increases during infection, and that KAT loss-of-function

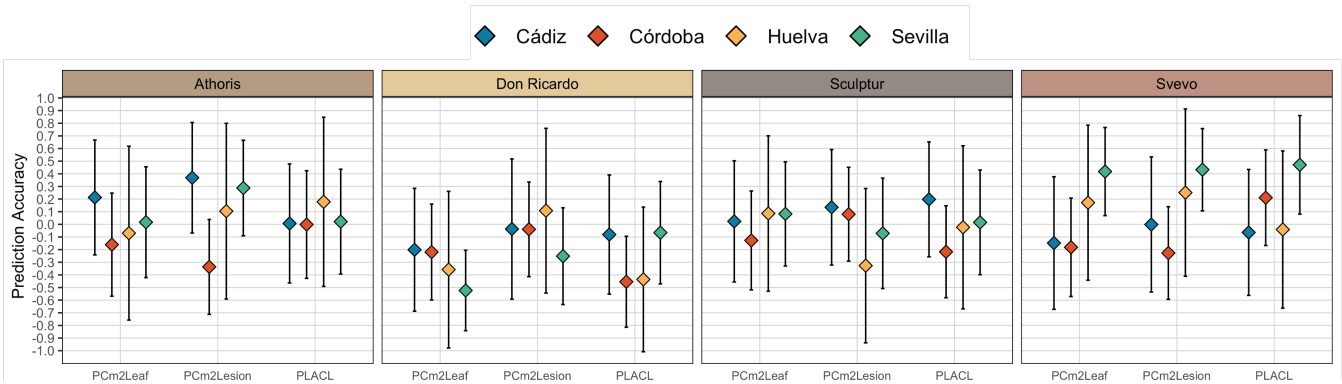

Fig. 6: **Within-region prediction accuracy**. Mean and standard deviation for each region-trait-cultivar combination after 500 rounds of Cross-Validation.

mutants exhibit reduced effector expression due to decreased histone acetylation. However, their analysis did not include the Rtt109 homolog *ZtIPO323_088990*. Based on our findings, this protein may positively regulate pycnidia formation, similar to two previously reported KATs. Thus, carrying the MTA could enhance histone acetyltransferase activity, potentially explaining the increased number of pycnidia per lesion surface in these strains. Furthermore, we speculate that *ZtIPO323_006440*, another KAT identified in our study, could also contribute to pycnidia production, reinforcing the role of histone acetylation in *Z. tritici* virulence.

Additionally, we identified a significant marker in the intergenic region between the fourth and fifth exons of *ZtIPO323_059020*, a Major Facilitator Superfamily (MFS) transporter with 12 predicted transmembrane domains. MFS proteins play key roles in nutrient uptake, effector secretion, and defense against plant-derived toxins (Pao et al., 1998). Previous GWAS studies in *Z. tritici* have associated genetic markers near MFS proteins with virulence (Zhong et al., 2017; Hartmann et al., 2017). While transmembrane proteins are often overlooked in effector predictions, accumulating evidence supports their involvement in fungal pathogenicity, with some functioning as virulence factors (Stergiopoulos et al., 2003; Oh et al., 2008). Our findings further reinforce this hypothesis.

Furthermore, we identified a polyketide synthase (PKS), *ZtIPO323_124400*, a key enzyme involved in the synthesis of polyketides, a major class of fungal secondary metabolites essential for plant pathogenicity (Rollini, 2002). A PKS producing (R)-miellin, a non-host-specific phytotoxin, was highly expressed in *Parastagonospora nodorum*, the causal agent of Septoria nodorum blotch (SNB) in wheat (Chooi et al., 2015). Similarly, a large PKS was identified as the avirulence gene *ACE1* in *Magnaporthe grisea*, recognized by resistant *Oryza sativa* cultivars. Given these findings, we hypothesize that *ZtIPO323_124400* may play a similar role in this pathosystem, contributing to fungal pathogenicity.

Consistent with previous studies (Amezrou et al., 2024), only two of the differentially expressed proteins were predicted to be secreted, highlighting the importance of non-secretory pathways in STB. However, further investigation is needed to determine how these proteins influence disease progression and to elucidate their molecular mechanisms.

Genomic Prediction

Prediction accuracy was highly dependent on the plant-pathogen combination. However, differences among wheat individuals (8.6–19.21%) had a greater impact than fungal mixes (0.18–1.82%), suggesting that wheat genotype plays a more significant role than pathogen variation. Incorporating host-pathogen interactions consistently improved prediction accuracy and explained a substantial portion of genetic variance, sometimes exceeding the combined variance of the host and pathogen. Unlike other pathosystems (Hudson et al., 2024), these interactions reduced overall genetic variance, emphasizing the importance of non-additive effects in disease severity. This highlights the specificity of the wheat-Z. tritici interaction and emphasizes the need for further exploration of non-additive genetic effects, such as dominance, in future studies.

Weighted models failed to outperform conventional genomic selection (GS) models, contradicting previous findings (Odilbekov et al., 2019; Alemu et al., 2021; Zakieh et al., 2023). This loss of accuracy may be due to the low number of significant GWAS hits. Additionally, incorporating GWAS markers as fixed effects reduced the influence of wheat and fungal genetic factors, likely because fixed effects dominated the response, diminishing the contribution of random genetic variation.

In 10 out of 16 models, error variance accounted for at least 80%, highlighting the complexity of modeling disease severity. The only exceptions were models incorporating non-additive host-pathogen interactions, where error variance dropped below 50% in one case (I/G model in Standard+I). This suggests that factors beyond genomic data, such as environmental variation, sample size, and measurement errors, introduce substantial noise.

Virulence predictions for *Z. tritici* remained unreliable, with high variability and frequent negative estimates. This suggests that fungal virulence cannot be predicted solely from genotypic data. Instead, the wheat genotype plays a dominant role in disease progression, aligning with our GS models where wheat variance consistently exceeded pathogen variance. Future studies should increase sample sizes to improve statistical power and clarify the genetic basis of *Z. tritici* virulence.

Consistent with previous studies, our GWAS provide strong evidence for host specificity in the *Z. tritici*-wheat pathosystem. In the GWAS analysis, none of the regions significantly associated with responses to different fungal mixes overlapped, suggesting

that each mix harbors distinct virulence mechanisms that trigger unique host responses. Similarly, no overlapping regions were detected in the pathogen GWAS, indicating that *Z. tritici* develops specific adaptations to each host, which acts as a selective environment. The strong isolate × cultivar interaction was further confirmed through GS modeling, where prediction accuracies based on wheat genotypes varied significantly depending on the specific isolate-cultivar combination (6). Additionally, virulence predictions differed across regions, suggesting that strains from each region interact differently with individual cultivars. This interaction underscores the challenges of predicting STB severity solely from fungal genomic data, highlighting the complexity of host-pathogen dynamics in this system.

Conclusion

This study advances our understanding of the genetic basis of wheat resistance to *Zymoseptoria tritici* and the pathogen's virulence strategies. By integrating host and pathogen genomic data, we identified novel fungal candidate genes, including a potential effector (*ZtIPO323_000490*), a histone acetyltransferase (*ZtIPO323_088990*), and a polyketide synthase (*ZtIPO323_124400*), suggesting roles for epigenetic regulation and secondary metabolites in pathogenicity. In wheat, we detected two putative QTL on chromosomes 1A and 4B linked to STB resistance. GWAS revealed strong isolate × cultivar specificity, with no overlapping resistance markers across fungal mixes or hosts. Key defense-related genes associated with MTAs included receptor-like kinases (*Kukri_c43701_385*, *Excalibur_c3683_328*), a glycosyltransferase on chromosome 6B, and zinc finger and B3 domain-containing transcription factors, providing valuable targets for resistance breeding. Genomic selection models incorporating pathogen data improved prediction accuracy in some cases, particularly when accounting for host-pathogen interactions. However, their variable performance highlights the complexity of virulence prediction and the need for larger, more diverse datasets. This study identifies key genetic factors in wheat resistance and *Z. tritici* pathogenicity, offering new targets for breeding more durable STB-resistant wheat varieties. Future research should focus on functional validation, refined prediction models, and multi-environment trials to enhance breeding strategies.

Competing interests

No competing interest is declared.

Author contributions statement

JIyS conceived the study and contributed to manuscript writing. ADR conducted the statistical analyses, prepared the figures, and wrote the manuscript. JIyS, ASV..... designed the experimental setup..... All authors reviewed and approved the final manuscript. We should be thinking of including Agrovegetal?

Funding

JIyS and ADR were supported by grant PID2021-123718OB-I00 funded by MCIN/AEI/10.13039/501 100 011 033 and by "ERDF A way of making Europe,CEX2020-000999-S. J.I.y.S was also supported by the Severo Ochoa Program for Centers of Excellence in R&D from the "Agencia Estatal de Investigación" of Spain to the CBGP. ADD info Lineas estratégicas

Acknowledgments

The authors thank the anonymous reviewers for their valuable suggestions. This work is supported in part by funds from the National Science Foundation (NSF: # 1636933 and # 1920920).

References

A. Alemu, G. Brazauskas, D. S. Gaikpa, T. Henriksson, B. Islamov, L. N. Jørgensen, M. Koppel, R. Koppel, Liatukas, J. T. Svensson, and A. Chawade. Genome-wide association analysis and genomic prediction for adult-plant resistance to septoria tritici blotch and powdery mildew in winter wheat. *Frontiers in Genetics*, 12, May 2021. ISSN 1664-8021. doi: 10.3389/fgene.2021.661742. URL http://dx.doi.org/10.3389/fgene.2021.661742.

R. Amezrou, C. Audéon, J. Compain, S. Gélisse, A. Ducasse, C. Saintenac, N. Lapalu, C. Louet, S. Orford, D. Croll, J. Amselem, S. Fillinger, and T. C. Marcel. A secreted protease-like protein in zymoseptoria tritici is responsible for avirulence on stb9 resistance gene in wheat. *PLOS Pathogens*, 19(5): e1011376, May 2023. ISSN 1553-7374. doi: 10.1371/journal.ppat.1011376. URL http://dx.doi.org/10.1371/journal.ppat.1011376.

R. Amezrou, A. Ducasse, J. Compain, N. Lapalu, A. Pitarch, L. Dupont, J. Confais, H. Goyeau, G. H. J. Kema, D. Croll, J. Amselem, A. Sanchez-Vallet, and T. C. Marcel. Quantitative pathogenicity and host adaptation in a fungal plant pathogen revealed by whole-genome sequencing. *Nature Communications*, 15(1), Mar. 2024. ISSN 2041-1723. doi: 10.1038/s41467-024-46191-1. URL http://dx.doi.org/10.1038/s41467-024-46191-1.

K. Ando, S. Rynearson, K. T. Muleta, J. Gedamu, B. Girma, N. A. Bosque-Pérez, M.-S. Chen, and M. O. Pumphrey. Genome-wide associations for multiple pest resistances in a northwestern united states elite spring wheat panel. *PLOS ONE*, 13(2): e0191305, Feb. 2018. ISSN 1932-6203. doi: 10.1371/journal.pone.0191305. URL http://dx.doi.org/10.1371/journal.pone.0191305.

C. Bartoli and F. Roux. Genome-wide association studies in plant pathosystems: Toward an ecological genomics approach. *Frontiers in Plant Science*, 8, May 2017. ISSN 1664-462X. doi: 10.3389/fpls.2017.00763. URL http://dx.doi.org/10.3389/fpls.2017.00763.

A. Bateman, M.-J. Martin, S. Orchard, M. Magrane, A. Adesina, S. Ahmad, E. H. Bowler-Barnett, H. Bye-A-Jee, D. Carpentier, P. Denny, J. Fan, P. Garmiri, L. J. d. C. Gonzales, A. Hussein, A. Ignatchenko, G. Insana, R. Ishtiaq, V. Joshi, D. Jyothi, S. Kandasaamy, A. Lock, A. Luciani, J. Luo, Y. Lussi, J. S. M. Marin, P. Raposo, D. L. Rice, R. Santos, E. Speretta, J. Stephenson, P. Totoo, N. Tyagi, N. Urakova, P. Vasudev, K. Warner, S. Wijerathne, C. W.-H. Yu, R. Zaru, A. J. Bridge, L. Aimo, G. Argoud-Puy, A. H. Auchincloss, K. B. Axelsen, P. Bansal, D. Baratin, T. M. Batista Neto, M.-C. Blatter, J. T. Bolleman, E. Boutet, L. Breuza, B. C. Gil, C. Casals-Casas, K. C. Echioukh, E. Coudert, B. Cuche, E. de Castro, A. Estreicher, M. L. Famiglietti, M. Feuermann, E. Gasteiger, P. Gaudet, S. Gehant, V. Gerritsen, A. Gos, N. Gruaz, C. Hulo, N. Hyka-Nouspikel, F. Jungo, A. Kerhornou, P. L. Mercier, D. Lieberherr, P. Masson, A. Morgat, S. Paesano, I. Pedruzzi, S. Pilbout, L. Pourcel, S. Poux, M. Pozzato, M. Pruess, N. Redaschi, C. Rivoire, C. J. A. Sigrist, K. Sonesson, S. Sundaram, A. Sveshnikova, C. H. Wu, C. N. Arighi, C. Chen, Y. Chen, H. Huang, K. Laiho, M. Lehvaslaiho, P. McGarvey, D. A. Natale, K. Ross, C. R. Vinayaka, Y. Wang, and J. Zhang. Uniprot: the universal protein knowledgebase in 2025. *Nucleic Acids Research*, 53(D1):D609–D617, Nov. 2024. ISSN 1362-4962. doi: 10.1093/nar/gkae1010. URL http://dx.doi.org/10.1093/nar/gkae1010.

D. Bates, M. Mächler, B. Bolker, and S. Walker. Fitting linear mixed-effects models usinglme4. *Journal of Statistical Software*, 67(1), 2015. ISSN 1548-7660. doi: 10.18637/jss.v067.i01. URL http://dx.doi.org/10.18637/jss.v067.i01.

R. Bernardo. Genomewide selection when major genes are known. *Crop Science*, 54(1):68–75, 2014.

M. Blum, A. Andreeva, L. Florentino, S. Chuguransky, T. Grego, E. Hobbs, B. Pinto, A. Orr, T. Paysan-Lafosse, I. Ponamareva, G. Salazar, N. Bordin, P. Bork, A. Bridge, L. Colwell, J. Gough, D. Haft, I. Letunic, F. Llinares-López, A. Marchler-Bauer, L. Meng-Papaxanthos, H. Mi, D. Natale, C. Orengo, A. Pandurangan, D. Piovesan, C. Rivoire, C. A. Sigrist, N. Thanki, F. Thibaud-Nissen, P. Thomas, S. E. Tosatto, C. Wu, and A. Bateman. Interpro: the protein sequence classification resource in 2025. *Nucleic Acids Research*, 53(D1): D444–D456, Nov. 2024. ISSN 1362-4962. doi: 10.1093/nar/gkae1082. URL http://dx.doi.org/10.1093/nar/gkae1082.

A. M. Bolger, M. Lohse, and B. Usadel. Trimmomatic: a flexible trimmer for illumina sequence data. *Bioinformatics*, 30(15):2114–2120, Apr. 2014. ISSN 1367-4803. doi: 10.1093/bioinformatics/btu170. URL http://dx.doi.org/10.1093/bioinformatics/btu170.

J. K. Brown, L. Chartrain, P. Lasserre-Zuber, and C. Saintenac. Genetics of resistance to zymoseptoria tritici and applications to wheat breeding. *Fungal Genetics and Biology*, 79:33–41, June 2015. ISSN 1087-1845. doi: 10.1016/j.fgb.2015.04.017. URL http://dx.doi.org/10.1016/j.fgb.2015.04.017.

L. Chartrain, S. T. Berry, and J. K. M. Brown. Resistance of wheat line kavkaz-k4500 l.6.a.4 to septoria tritici blotch controlled by isolate-specific resistance genes. *Phytopathology®*, 95(6):664–671, June 2005. ISSN 1943-7684. doi: 10.1094/phyto-95-0664. URL http://dx.doi.org/10.1094/PHYTO-95-0664.

P. Cheval, A. Siah, M. Bomble, A. D. Popper, P. Reignault, and P. Halama. Evolution of qoi resistance of the wheat pathogen zymoseptoria tritici in northern france. *Crop Protection*, 92: 131–133, Feb. 2017. ISSN 0261-2194. doi: 10.1016/j.cropro.2016.10.017. URL http://dx.doi.org/10.1016/j.cropro.2016.10.017.

Y.-H. Chooi, C. Krill, R. A. Barrow, S. Chen, R. Trengove, R. P. Oliver, and P. S. Solomon. An in planta -expressed polyketide synthase produces (r)-mellein in the wheat pathogen parastagonospora nodorum. *Applied and Environmental Microbiology*, 81(1):177–186, Jan. 2015. ISSN 1098-5336. doi: 10.1128/aem.02745-14. URL http://dx.doi.org/10.1128/AEM.02745-14.

P. Cingolani, A. Platts, L. L. Wang, M. Coon, T. Nguyen, L. Wang, S. J. Land, X. Lu, and D. M. Ruden. A program for annotating and predicting the effects of single nucleotide polymorphisms, snpeff: Snps in the genome of drosophila melanogaster strain w1118; iso-2; iso-3. *Fly*, 6(2):80–92, Apr. 2012. ISSN 1933-6942. doi: 10.4161/fly.19695. URL http://dx.doi.org/10.4161/fly.19695.

A. Feurtey, C. Lorrain, M. C. McDonald, A. Milgate, P. S. Solomon, R. Warren, G. Puccetti, G. Scalliet, S. F. F. Torriani, L. Gout, T. C. Marcel, F. Suffert, J. Alassimone, A. Lipzen, Y. Yoshinaga, C. Daum, K. Barry, I. V. Grigoriev, S. B. Goodwin, A. Genissel, M. F. Seidl, E. H. Stukenbrock,

M.-H. Lebrun, G. H. J. Kema, B. A. McDonald, and D. Croll. A thousand-genome panel retraces the global spread and adaptation of a major fungal crop pathogen. *Nature Communications*, 14(1), Feb. 2023. ISSN 2041-1723. doi: 10.1038/s41467-023-36674-y. URL http://dx.doi.org/10.1038/s41467-023-36674-y.

H. Fones and S. Gurr. The impact of septoria tritici blotch disease on wheat: An eu perspective. *Fungal Genetics and Biology*, 79:3–7, June 2015. ISSN 1087-1845. doi: 10.1016/j.fgb.2015.04.004. URL http://dx.doi.org/10.1016/j.fgb.2015.04.004.

M. Freitag. Histone methylation by set domain proteins in fungi. *Annual Review of Microbiology*, 71(1):413–439, Sept. 2017. ISSN 1545-3251. doi: 10.1146/annurev-micro-102215-095757. URL http://dx.doi.org/10.1146/annurev-micro-102215-095757.

B. D. O. Geraldine A. Van der Auwera. *Genomics in the Cloud*. O'Reilly Media, O'Reilly Media, 04 2020. ISBN 9781491975169, 1491975164.

G. S. Gerard, A. Börner, U. Lohwasser, and M. R. Simón. Genome-wide association mapping of genetic factors controlling septoria tritici blotch resistance and their associations with plant height and heading date in wheat. *Euphytica*, 213(1), Jan. 2017. ISSN 1573-5060. doi: 10.1007/s10681-016-1820-1. URL http://dx.doi.org/10.1007/s10681-016-1820-1.

S. B. Goodwin, S. Ben M'Barek, B. Dhillon, A. H. J. Wittenberg, C. F. Crane, J. K. Hane, A. J. Foster, T. A. J. Van der Lee, J. Grimwood, A. Aerts, J. Antoniw, A. Bailey, B. Bluhm, J. Bowler, J. Bristow, A. van der Burgt, B. Canto-Canché, A. C. L. Churchill, L. Conde-Ferràez, H. J. Cools, P. M. Coutinho, M. Csukai, P. Dehal, P. De Wit, B. Donzelli, H. C. van de Geest, R. C. H. J. van Ham, K. E. Hammond-Kosack, B. Henrissat, A. Kilian, A. K. Kobayashi, E. Koopmann, Y. Kourmpetis, A. Kuzniar, E. Lindquist, V. Lombard, C. Maliepaard, N. Martins, R. Mehrabi, J. P. H. Nap, A. Ponomarenko, J. J. Rudd, A. Salamov, J. Schmutz, H. J. Schouten, H. Shapiro, I. Stergiopoulos, S. F. F. Torriani, H. Tu, R. P. de Vries, C. Waalwijk, S. B. Ware, A. Wiebenga, L.-H. Zwiers, R. P. Oliver, I. V. Grigoriev, and G. H. J. Kema. Finished genome of the fungal wheat pathogen mycosphaerella graminicola reveals dispensome structure, chromosome plasticity, and stealth pathogenesis. *PLoS Genetics*, 7(6):e1002070, June 2011. ISSN 1553-7404. doi: 10.1371/journal.pgen.1002070. URL http://dx.doi.org/10.1371/journal.pgen.1002070.

S. Gurung, S. Mamidi, J. M. Bonman, M. Xiong, G. Brown-Guedira, and T. B. Adhikari. Genome-wide association study reveals novel quantitative trait loci associated with resistance to multiple leaf spot diseases of spring wheat. *PLoS ONE*, 9(9):e108179, Sept. 2014. ISSN 1932-6203. doi: 10.1371/journal.pone.0108179. URL http://dx.doi.org/10.1371/journal.pone.0108179.

A. N. Hafeez, L. Chartrain, C. Feng, F. Cambon, M. Clarke, S. Griffiths, S. Hayta, M. Jiang, B. Keller, R. Kirby, M. C. Kolodziej, O. R. Powell, M. Smedley, B. Steuernagel, W. Xian, L. U. Wingen, S. Cheng, C. Saintenac, B. B. H. Wulff, and J. K. M. Brown. Septoria tritici blotch resistance genestb15encodes a lectin receptor-like kinase. *Biorxiv*, Sept. 2023. doi: 10.1101/2023.09.11.557217. URL http://dx.doi.org/10.1101/2023.09.11.557217.

J. Hallgren, K. D. Tsirigos, M. D. Pedersen, J. J. Almagro Armenteros, P. Marcatili, H. Nielsen, A. Krogh, and O. Winther. Deeptmhmm predicts alpha and beta transmembrane proteins using deep neural networks. *Biorxiv*, Apr. 2022. doi: 10.1101/2022.04.08.487609. URL http://dx.doi.org/10.1101/2022.04.08.487609.

W. Hansberg, R. Salas-Lizana, and L. Domínguez. Fungal catalases: Function, phylogenetic origin and structure. *Archives of Biochemistry and Biophysics*, 525(2):170–180, Sept. 2012. ISSN 0003-9861. doi: 10.1016/j.abb.2012.05.014. URL http://dx.doi.org/10.1016/j.abb.2012.05.014.

F. E. Hartmann, A. Sánchez-Vallet, B. A. McDonald, and D. Croll. A fungal wheat pathogen evolved host specialization by extensive chromosomal rearrangements. *The ISME Journal*, 11 (5):1189–1204, Jan. 2017. ISSN 1751-7370. doi: 10.1038/ismej.2016.196. URL http://dx.doi.org/10.1038/ismej.2016.196.

Y. He, D. Ahmad, X. Zhang, Y. Zhang, L. Wu, P. Jiang, and H. Ma. Genome-wide analysis of family-1 udp glycosyltransferases (ugt) and identification of ugt genes for fhb resistance in wheat (triticum aestivum l.). *BMC Plant Biology*, 18(1), Apr. 2018. ISSN 1471-2229. doi: 10.1186/s12870-018-1286-5. URL http://dx.doi.org/10.1186/s12870-018-1286-5.

W. Hill and B. Weir. Variances and covariances of squared linkage disequilibria in finite populations. *Theoretical Population Biology*, 33(1):54–78, Feb. 1988. ISSN 0040-5809. doi: 10.1016/0040-5809(88)90004-4. URL http://dx.doi.org/10.1016/0040-5809(88)90004-4.

M. Huang, X. Liu, Y. Zhou, R. M. Summers, and Z. Zhang. Blink: a package for the next level of genome-wide association studies with both individuals and markers in the millions. *GigaScience*, 8(2), Dec. 2018. ISSN 2047-217X. doi: 10.1093/gigascience/giy154. URL http://dx.doi.org/10.1093/gigascience/giy154.

O. Hudson, M. F. R. Resende, C. Messina, J. Holland, and J. Brawner. Prediction of resistance, virulence, and host-by-pathogen interactions using dual-genome prediction models. *Theoretical and Applied Genetics*, 137(8), Aug. 2024. ISSN 1432-2242. doi: 10.1007/s00122-024-04698-7. URL http://dx.doi.org/10.1007/s00122-024-04698-7.

J. Isidro, D. Akdemir, and J. Burke. Genomic selection. In A. William, B. Alain, and V. G. Maarten, editors, *The world wheat book: a history of wheat breeding*, volume 3, chapter 32, pages 1001–1023. Lavoisier,Paris, 2016.

G. H. J. Kema, A. Mirzadi Gohari, L. Aouini, H. A. Y. Gibriel, S. B. Ware, F. van den Bosch, R. Manning-Smith, V. Alonso-Chavez, J. Helps, S. Ben M'Barek, R. Mehrabi, C. Diaz-Trujillo, E. Zamani, H. J. Schouten, T. A. J. van der Lee, C. Waalwijk, M. A. de Waard, P. J. G. M. de Wit, E. C. P. Verstappen, B. P. H. J. Thomma, H. J. G. Meijer, and M. F. Seidl. Stress and sexual reproduction affect the dynamics of the wheat pathogen effector avrstb6 and strobilurin resistance. *Nature Genetics*, 50(3):375–380, Feb. 2018. ISSN 1546-1718. doi: 10.1038/s41588-018-0052-9. URL http://dx.doi.org/10.1038/s41588-018-0052-9.

S. Kollers, B. Rodemann, J. Ling, V. Korzun, E. Ebmeyer, O. Argillier, M. Hinze, J. Plieske, D. Kulosa, M. W. Ganal, and M. S. Röder. Whole genome association mapping of fusarium head blight resistance in european winter wheat (triticum aestivum l.). *PLoS ONE*, 8(2):e57500, Feb. 2013. ISSN 1932-6203. doi: 10.1371/journal.pone.0057500. URL http://dx.doi.org/10.1371/journal.pone.0057500.

N. Lapalu, L. Lamothe, Y. Petit, A. Genissel, C. Delude, A. Feurtey, L. N. Abraham, D. Smith, R. King, A. Renwick, M. Appertet, J. Sucher, A. S. Steindorff, S. B. Goodwin, G. H. Kema, I. V. Grigoriev, J. Hane, J. Rudd, E. Stukenbrock, D. Croll, G. Scalliet, and M.-H. Lebrun. Improved gene annotation of the fungal wheat pathogenzymoseptoria triticibased on combined iso-seq and rna-seq evidence. *Biorxiv*, Apr. 2023. doi: 10.1101/2023.04.26.537486. URL `http://dx.doi.org/10.1101/2023.04.26.537486`.

H. Li and R. Durbin. Fast and accurate short read alignment with burrows–wheeler transform. *Bioinformatics*, 25(14):1754–1760, May 2009. ISSN 1367-4803. doi: 10.1093/bioinformatics/btp324. URL `http://dx.doi.org/10.1093/bioinformatics/btp324`.

H. Li, B. Handsaker, A. Wysoker, T. Fennell, J. Ruan, N. Homer, G. Marth, G. Abecasis, and R. Durbin. The sequence alignment/map format and samtools. *Bioinformatics*, 25(16):2078–2079, June 2009. ISSN 1367-4803. doi: 10.1093/bioinformatics/btp352. URL `http://dx.doi.org/10.1093/bioinformatics/btp352`.

W.-T. Li, M. He, J. Wang, and Y.-P. Wang. Zinc finger protein (zfp) in plants-a review. *Plant Omics*, 6(6), 2013.

A. E. Lipka, F. Tian, Q. Wang, J. Peiffer, M. Li, P. J. Bradbury, M. A. Gore, E. S. Buckler, and Z. Zhang. Gapit: genome association and prediction integrated tool. *Bioinformatics*, 28(18):2397–2399, July 2012. ISSN 1367-4803. doi: 10.1093/bioinformatics/bts444. URL `http://dx.doi.org/10.1093/bioinformatics/bts444`.

X. Liu, M. Huang, B. Fan, E. S. Buckler, and Z. Zhang. Iterative usage of fixed and random effect models for powerful and efficient genome-wide association studies. *PLOS Genetics*, 12(2):e1005767, Feb. 2016. ISSN 1553-7404. doi: 10.1371/journal.pgen.1005767. URL `http://dx.doi.org/10.1371/journal.pgen.1005767`.

S. Louriki, S. Rehman, S. El Hanafi, Y. Bouhouch, M. Al-Jaboobi, A. Amri, A. Douira, and W. Tadesse. Identification of resistance sources and genome-wide association mapping of septoria tritici blotch resistance in spring bread wheat germplasm of icarda. *Frontiers in Plant Science*, 12, May 2021. ISSN 1664-462X. doi: 10.3389/fpls.2021.600176. URL `http://dx.doi.org/10.3389/fpls.2021.600176`.

L. Meile, D. Croll, P. C. Brunner, C. Plissonneau, F. E. Hartmann, B. A. McDonald, and A. Sánchez-Vallet. A fungal avirulence factor encoded in a highly plastic genomic region triggers partial resistance to septoria tritici blotch. *New Phytologist*, 219(3):1048–1061, Apr. 2018. ISSN 1469-8137. doi: 10.1111/nph.15180. URL `http://dx.doi.org/10.1111/nph.15180`.

T. Mekonnen, C. H. Sneller, T. Haileselassie, C. Ziyomo, B. G. Abeyo, S. B. Goodwin, D. Lule, and K. Tesfaye. Genome-wide association study reveals novel genetic loci for quantitative resistance to septoria tritici blotch in wheat (triticum aestivum l.). *Frontiers in Plant Science*, 12, Sept. 2021. ISSN 1664-462X. doi: 10.3389/fpls.2021.671323. URL `http://dx.doi.org/10.3389/fpls.2021.671323`.

T. H. E. Meuwissen, B. J. Hayes, and M. E. Goddard. Prediction of total genetic value using genome-wide dense marker maps. *Genetics*, 157(4):1819–1829, Apr. 2001. ISSN 1943-2631. doi: 10.1093/genetics/157.4.1819. URL `http://dx.doi.org/10.1093/genetics/157.4.1819`.

A. Mirzadi Gohari, R. Mehrabi, S. Kilaru, M. Schuster, G. Steinberg, P. P. J. G. M. de Wit, and G. H. J. Kema. Functional characterization of extracellular and intracellular catalase-peroxidases involved in virulence of the fungal wheat pathogen zymoseptoria tritici. *Molecular Plant Pathology*, 25 (10), Oct. 2024. ISSN 1364-3703. doi: 10.1111/mpp.70009. URL `http://dx.doi.org/10.1111/mpp.70009`.

J. Mistry, S. Chuguransky, L. Williams, M. Qureshi, G. Salazar, E. L. L. Sonnhammer, S. C. E. Tosatto, L. Paladin, S. Raj, L. J. Richardson, R. D. Finn, and A. Bateman. Pfam: The protein families database in 2021. *Nucleic Acids Research*, 49 (D1):D412–D419, Oct. 2020. ISSN 1362-4962. doi: 10.1093/nar/gkaa913. URL `http://dx.doi.org/10.1093/nar/gkaa913`.

Q. H. Muqaddasi, Y. Zhao, B. Rodemann, J. Plieske, M. W. Ganal, and M. S. Röder. Genome-wide association mapping and prediction of adult stage septoria tritici blotch infection in european winter wheat via high-density marker arrays. *The Plant Genome*, 12(1), Mar. 2019. ISSN 1940-3372. doi: 10.3835/plantgenome2018.05.0029. URL `http://dx.doi.org/10.3835/plantgenome2018.05.0029`.

F. Odilbekov, R. Armonienė, A. Koc, J. Svensson, and A. Chawade. Gwas-assisted genomic prediction to predict resistance to septoria tritici blotch in nordic winter wheat at seedling stage. *Frontiers in Genetics*, 10, Nov. 2019. ISSN 1664-8021. doi: 10.3389/fgene.2019.01224. URL `http://dx.doi.org/10.3389/fgene.2019.01224`.

Y. Oh, N. Donofrio, H. Pan, S. Coughlan, D. E. Brown, S. Meng, T. Mitchell, and R. A. Dean. Transcriptome analysis reveals new insight into appressorium formation and function in the rice blast fungus magnaporthe oryzae. *Genome Biology*, 9(5), May 2008. ISSN 1474-760X. doi: 10.1186/gb-2008-9-5-r85. URL `http://dx.doi.org/10.1186/gb-2008-9-5-r85`.

S. S. Pao, I. T. Paulsen, and M. H. Saier. Major facilitator superfamily. *Microbiology and Molecular Biology Reviews*, 62 (1):1–34, Mar. 1998. ISSN 1098-5557. doi: 10.1128/mmbr.62.1.1-34.1998. URL `http://dx.doi.org/10.1128/mmbr.62.1.1-34.1998`.

D. Piaskowska, U. Piechota, M. Radecka-Janusik, and P. Czembor. Qtl mapping of seedling and adult plant resistance to septoria tritici blotch in winter wheat cv. mandub (triticum aestivum l.). *Agronomy*, 11(6):1108, May 2021. ISSN 2073-4395. doi: 10.3390/agronomy11061108. URL `http://dx.doi.org/10.3390/agronomy11061108`.

S. Purcell, B. Neale, K. Todd-Brown, L. Thomas, M. A. Ferreira, D. Bender, J. Maller, P. Sklar, P. I. de Bakker, M. J. Daly, and P. C. Sham. Plink: A tool set for whole-genome association and population-based linkage analyses. *The American Journal of Human Genetics*, 81(3):559–575, Sept. 2007. ISSN 0002-9297. doi: 10.1086/519795. URL `http://dx.doi.org/10.1086/519795`.

P. Pérez and G. de los Campos. Genome-wide regression and prediction with the bglr statistical package. *Genetics*, 198(2):483–495, July 2014. ISSN 1943-2631. doi: 10.1534/genetics.114.164442. URL `http://dx.doi.org/10.1534/genetics.114.164442`.

A. Riaz, P. KockAppelgren, J. G. Hehir, J. Kang, F. Meade, J. Cockram, D. Milbourne, J. Spink, E. Mullins, and S. Byrne. Genetic analysis using a multi-parent wheat population identifies novel sources of septoria tritici blotch resistance. *Genes*, 11(8):887, Aug. 2020. ISSN 2073-4425. doi: 10.3390/genes11080887. URL `http://dx.doi.org/10.3390/genes11080887`.

M. Rollini, M. Manzoni. Biosynthesis and biotechnological production of statins by filamentous fungi and application of these cholesterol-lowering drugs. *Applied Microbiology and Biotechnology*, 58(5):555–564, Apr. 2002. ISSN 1432-0614 doi: 10.1007/s00253-002-0932-9. URL http://dx.doi.org/10.1007/s00253-002-0932-9.

S. B. Rothbart and B. D. Strahl. Interpreting the language of histone and dna modifications. *Biochimica et Biophysica Acta (BBA) - Gene Regulatory Mechanisms*, 1839(8):627–643, Aug 2014. ISSN 1874-9399. doi: 10.1016/j.bbagrm.2014.03.001. URL http://dx.doi.org/10.1016/j.bbagrm.2014.03.001.

C. Saintenac, W.-S. Lee, F. Cambon, J. J. Rudd, R. C King, W. Marande, S. J. Powers, H. Bergès, A. L. Phillips C. Uauy, K. E. Hammond-Kosack, T. Langin, and K. Kanyuka Wheat receptor-kinase-like protein stb6 controls gene-for-gene resistance to fungal pathogen zymoseptoria tritici. *Nature Genetics*, 50(3):368–374, Feb. 2018. ISSN 1546-1718. doi: 10 1038/s41588-018-0051-x. URL http://dx.doi.org/10.1038/s41588-018-0051-x.

C. Saintenac, F. Cambon, L. Aouini, E. Verstappen, S. M. T Ghaffary, T. Poucet, W. Marande, H. Berges, S. Xu M. Jaouannet, B. Favery, J. Alassimone, A. Sánchez-Vallet J. Faris, G. Kema, O. Robert, and T. Langin. A wheat cysteine- rich receptor-like kinase confers broad-spectrum resistance against septoria tritici blotch. *Nature Communications*, 12(1) Jan. 2021. ISSN 2041-1723. doi: 10.1038/s41467-020-20685-0 URL http://dx.doi.org/10.1038/s41467-020-20685-0.

S. Savary, L. Willocquet, S. J. Pethybridge, P. Esker N. McRoberts, and A. Nelson. The global burden of pathogens and pests on major food crops. *Nature Ecology amp; Evolution*, 3(3):430–439, Feb. 2019. ISSN 2397-334X doi: 10.1038/s41559-018-0793-y. URL http://dx.doi.org/10.1038/s41559-018-0793-y.

J.-H. Shin, S. Blay, J. Graham, and B. McNeney. Ldheatmap Anrfunction for graphical display of pairwise linkage disequilibria between single nucleotide polymorphisms *Journal of Statistical Software*, 16(Code Snippet 3) 2006. ISSN 1548-7660. doi: 10.18637/jss.v016.c03. URL http://dx.doi.org/10.18637/jss.v016.c03.

J. Sperschneider and P. N. Dodds. Effectorp 3.0: Prediction of apoplastic and cytoplasmic effectors in fungi and oomycetes *Molecular Plant-Microbe Interactions®*, 35(2):146–156, Feb 2022. ISSN 1943-7706. doi: 10.1094/mpmi-08-21-0201-r. URL http://dx.doi.org/10.1094/MPMI-08-21-0201-R.

J. E. Spindel, H. Begum, D. Akdemir, B. Collard, E. Redoña, J.-L Jannink, and S. McCouch. Genome-wide prediction models that incorporate de novo gwas are a powerful new tool for tropical rice improvement. *Heredity*, 116(4):395–408, Feb. 2016. ISSN 1365-2540. doi: 10.1038/hdy.2015.113. URL http://dx.doi.org/10.1038/hdy.2015.113.

I. Stergiopoulos, L.-H. Zwiers, and M. A. De Waard. The abc transporter mgatr4 is a virulence factor of mycosphaerella graminicola that affects colonization of substomatal cavities in wheat leaves. *Molecular Plant-Microbe Interactions®*, 16(8) 689–698, Aug. 2003. ISSN 1943-7706. doi: 10.1094/mpmi.2003 16.8.689. URL http://dx.doi.org/10.1094/mpmi.2003.16.8.689.

M. Suarez-Fernandez, R. Álvarez Aragón, A. Pastor-Mediavilla A. Maestre-Guillén, I. del Olmo, A. De Francesco, L. Meile, and A. Sánchez-Vallet. Sas3-mediated histone acetylation regulates effector gene activation in a fungal plant pathogen. *mBio*, 14 (5), Oct. 2023. ISSN 2150-7511. doi: 10.1128/mbio.01386-23. URL http://dx.doi.org/10.1128/mbio.01386-23.

F. Sun, X. Liu, Q. Wei, J. Liu, T. Yang, L. Jia, Y. Wang, G. Yang, and G. He. Functional characterization of tafusca3, a b3-superfamily transcription factor gene in the wheat. *Frontiers in Plant Science*, 8, June 2017. ISSN 1664-462X. doi: 10.3389/fpls.2017.01133. URL http://dx.doi.org/10.3389/fpls.2017.01133.

A. Sánchez-Vallet, F. E. Hartmann, T. C. Marcel, and D. Croll. Nature's genetic screens: using genome-wide association studies for effector discovery. *Molecular Plant Pathology*, 19(1):3–6, Dec. 2017. ISSN 1364-3703. doi: 10.1111/mpp.12592. URL http://dx.doi.org/10.1111/mpp.12592.

F. Teufel, J. J. Almagro Armenteros, A. R. Johansen, M. H. Gíslason, S. I. Pihl, K. D. Tsirigos, O. Winther, S. Brunak, G. von Heijne, and H. Nielsen. Signalp 6.0 predicts all five types of signal peptides using protein language models. *Nature Biotechnology*, 40(7):1023–1025, Jan. 2022. ISSN 1546-1696. doi: 10.1038/s41587-021-01156-3. URL http://dx.doi.org/10.1038/s41587-021-01156-3.

J.-N. Thauvin, S. Gélisse, F. Cambon, T. Langin, T. C. Marcel, and C. Saintenac. The genetic architecture of resistance to septoria tritici blotch in french wheat cultivars. *BMC Plant Biology*, 24(1), Dec. 2024. ISSN 1471-2229. doi: 10.1186/s12870-024-05898-5. URL http://dx.doi.org/10.1186/s12870-024-05898-5.

S. F. Torriani, J. P. Melichar, C. Mills, N. Pain, H. Sierotzki, and M. Courbot. Zymoseptoria tritici: A major threat to wheat production, integrated approaches to control. *Fungal Genetics and Biology*, 79:8–12, June 2015. ISSN 1087-1845. doi: 10.1016/j.fgb.2015.04.010. URL http://dx.doi.org/10.1016/j.fgb.2015.04.010.

N. Vagndorf, N. H. Nielsen, V. Edriss, J. R. Andersen, J. Orabi, L. N. Jørgensen, and A. Jahoor. Genomewide association study reveals novel quantitative trait loci associated with resistance towards septoria tritici blotch in north european winter wheat. *Plant Breeding*, 136(4):474–482, June 2017. ISSN 1439-0523. doi: 10.1111/pbr.12490. URL http://dx.doi.org/10.1111/pbr.12490.

S. Wang, D. Wong, K. Forrest, A. Allen, S. Chao, B. E. Huang, M. Maccaferri, S. Salvi, S. G. Milner, L. Cattivelli, A. M. Mastrangelo, A. Whan, S. Stephen, G. Barker, R. Wieseke, J. Plieske, M. Lillemo, D. Mather, R. Appels, R. Dolferus, G. Brown-Guedira, A. Korol, A. R. Akhunova, C. Feuillet, J. Salse, M. Morgante, C. Pozniak, M. Luo, J. Dvorak, M. Morell, J. Dubcovsky, M. Ganal, R. Tuberosa, C. Lawley, I. Mikoulitch, C. Cavanagh, K. J. Edwards, M. Hayden, and E. Akhunov. Characterization of polyploid wheat genomic diversity using a high-density 90 000 single nucleotide polymorphism array. *Plant Biotechnology Journal*, 12(6):787–796, Mar. 2014. ISSN 1467-7652. doi: 10.1111/pbi.12183. URL http://dx.doi.org/10.1111/pbi.12183.

T. Wang, C. Long, M. Chang, Y. Wu, S. Su, J. Wei, S. Jiang, X. Wang, J. He, D. Xing, Y. He, Y. Ran, and W. Li. Genome-wide identification of the b3 transcription factor family in pepper (capsicum annuum) and expression patterns during fruit ripening. *Scientific Reports*, 14(1), Jan. 2024. ISSN 2045-2322. doi: 10.1038/s41598-023-51080-6. URL http://dx.doi.org/10.1038/s41598-023-51080-6.

N. Yang, B. Ovenden, B. Baxter, M. C. McDonald, P. S. Solomon, and A. Milgate. Multi-stage resistance to zymoseptoria tritici

revealed by gwas in an australian bread wheat diversity panel. *Frontiers in Plant Science*, 13, Oct. 2022. ISSN 1664-462X. doi: 10.3389/fpls.2022.990915. URL http://dx.doi.org/10.3389/fpls.2022.990915.

S. Yates, A. Mikaberidze, S. G. Krattinger, M. Abrouk, A. Hund, K. Yu, B. Studer, S. Fouche, L. Meile, D. Pereira, P. Karisto, and B. A. McDonald. Precision phenotyping reveals novel loci for quantitative resistance to septoria tritici blotch. *Plant Phenomics*, 2019:3285904, 2019. ISSN 2643-6515. doi: 10.34133/2019/3285904. URL http://dx.doi.org/10.34133/2019/3285904.

L. Yin, H. Zhang, Z. Tang, J. Xu, D. Yin, Z. Zhang, X. Yuan, M. Zhu, S. Zhao, X. Li, and X. Liu. rmvp: A memory-efficient, visualization-enhanced, and parallel-accelerated tool for genome-wide association study. *Genomics, Proteomics amp; Bioinformatics*, 19(4):619–628, Mar. 2021. ISSN 2210-3244. doi: 10.1016/j.gpb.2020.10.007. URL http://dx.doi.org/10.1016/j.gpb.2020.10.007.

M. Zakieh, A. Alemu, T. Henriksson, N. Pareek, P. K. Singh, and A. Chawade. Exploring gwas and genomic prediction to improve septoria tritici blotch resistance in wheat. *Scientific Reports*, 13(1), Sept. 2023. ISSN 2045-2322. doi: 10.1038/s41598-023-42856-x. URL http://dx.doi.org/10.1038/s41598-023-42856-x.

Y. Zhang, D. Huai, Q. Yang, Y. Cheng, M. Ma, D. J. Kliebenstein, and Y. Zhou. Overexpression of three glucosinolate biosynthesis genes in brassica napus identifies enhanced resistance to sclerotinia sclerotiorum and botrytis cinerea. *PLoS One*, 10 (10):e0140491, Oct. 2015. URL http://creativecommons.org/licenses/by/4.0/.

Z. Zhong, T. C. Marcel, F. E. Hartmann, X. Ma, C. Plissonneau, M. Zala, A. Ducasse, J. Confais, J. Compain, N. Lapalu, J. Amselem, B. A. McDonald, D. Croll, and J. Palma-Guerrero. A small secreted protein in zymoseptoria tritici is responsible for avirulence on wheat cultivars carrying the stb6 resistance gene. *New Phytologist*, 214(2):619–631, Feb. 2017. ISSN 1469-8137. doi: 10.1111/nph.14434. URL http://dx.doi.org/10.1111/nph.14434.

Supplementary material

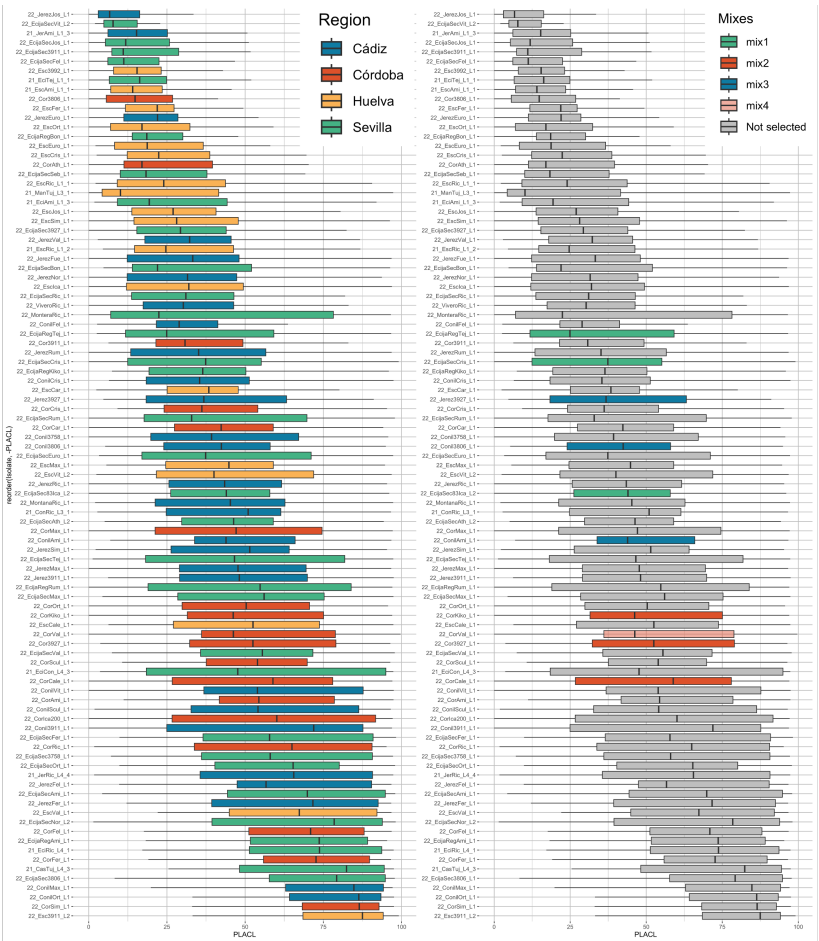

Fig. S1: **PLACL Distribution and Mixes Individuals**. The figure shows the Percentage of Leaf Area Covered by Lesions (PLACL) for 100 Z. tritici isolates across four hosts. Isolates are ranked from the least to the most pathogenic and are colored according to their region of extraction. The right panel details the isolates selected for the inoculum mixes: mix1 comprises *22_EcijaSec83Ica_L2*, *22_EcijaSecCris_L1*, and *22_EcijaRegTej_L1*; mix2 comprises *22_CorKiko_L1*, *22_CorCale_L1*, and *22_Cor3927_L1*; mix3 comprises *22_ConilAmi_L1*, *22_Conil3806_L1*, and 22_*Jerez3927_L1*; and mix4 consists of *22_CorVal_L1*.

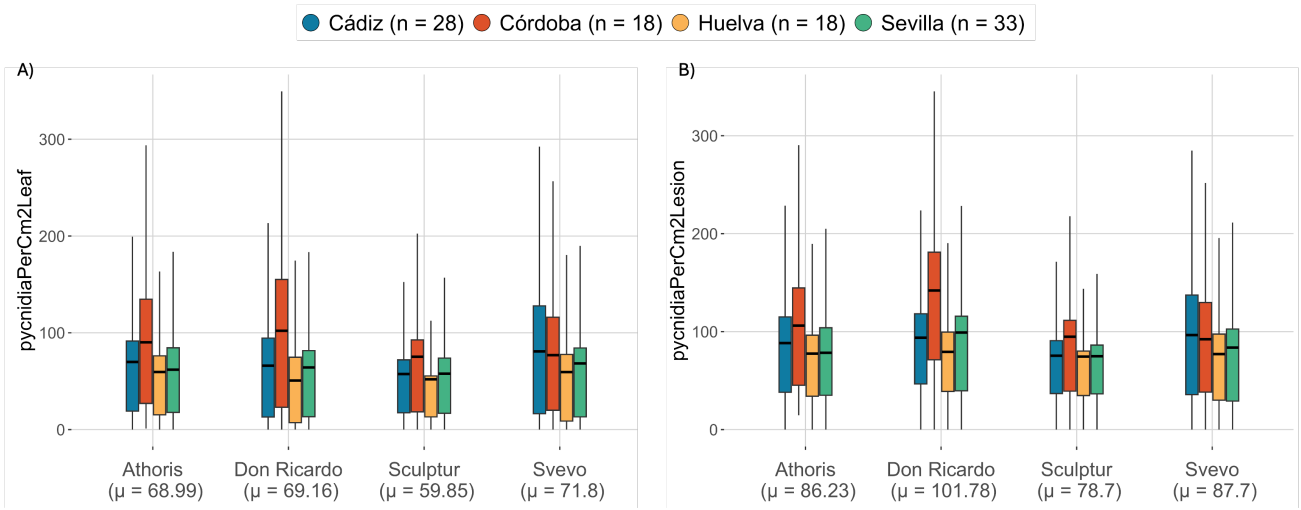

Fig. S2: **Phenotypic Distributions for PCm2Leaf and PCm2Lesions**. Boxplots display the distributions of PCm2Leaf and PCm2Lesions in 100 Zymoseptoria tritici isolates, grouped by region of extraction, illustrating variation in pycnidia traits.

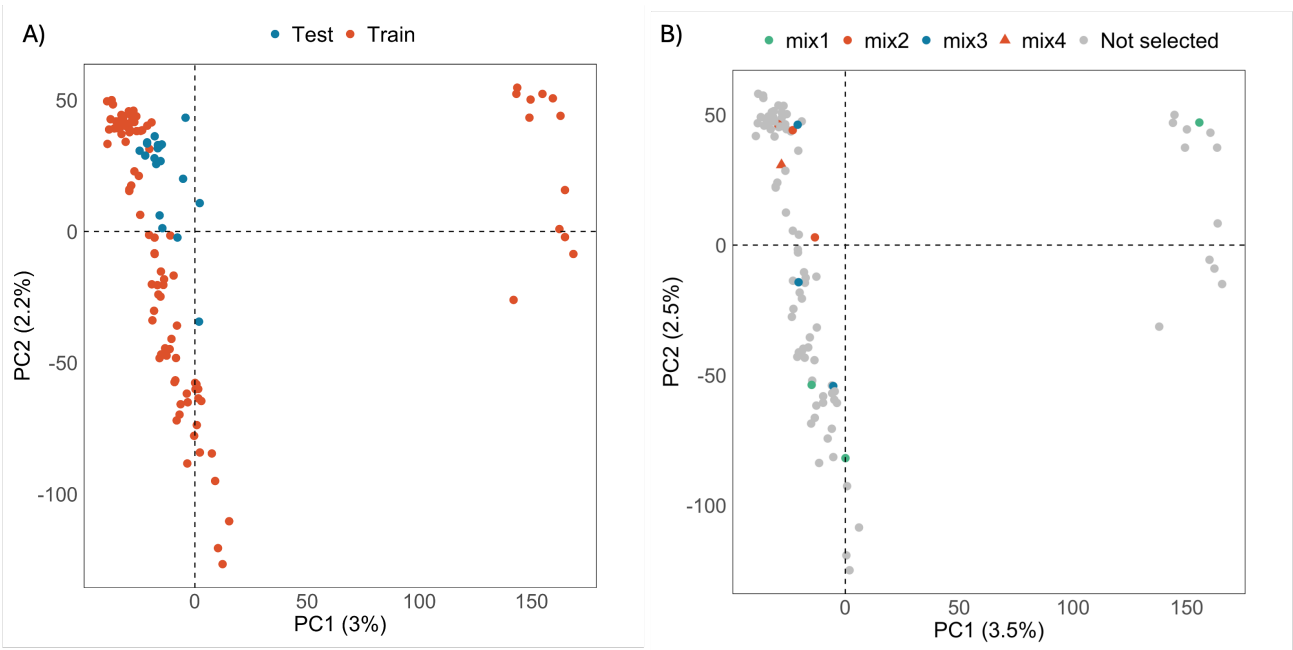

Fig. S3: **Principal Component Analysis of the Z. tritici Population**. A) shows a two-dimensional representation of the PCA for the fungal training and test populations (119 isolates). B displays the PCA coordinates for the isolates selected for each mix.

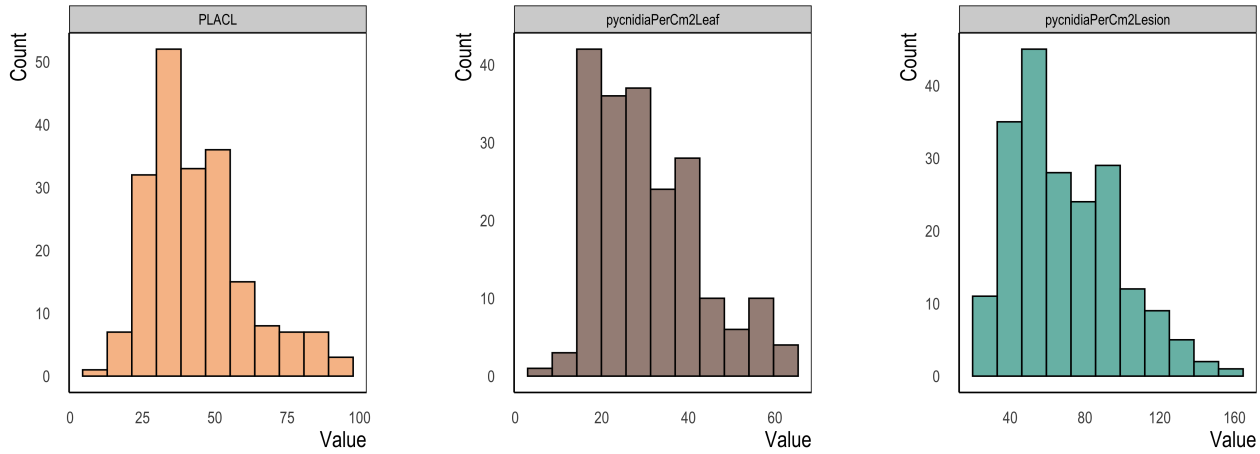

Fig. S4: **Histogram of adjusted phenotypes**. Distribution of Best Linear Unbiased Predictions for each Z.tritici isolate and trait

Chr	Length	n	Density	High	Low	Moderate	Modifier
1	6088797	114220	53.31	270 (0.2%)	40861 (35.8%)	13615 (11.9%)	59474 (52.1%)
2	3860111	63004	61.27	197 (0.3%)	23052 (36.6%)	7933 (12.6%)	31822 (50.5%)
3	3505381	62446	56.13	106 (0.2%)	23372 (37.4%)	7529 (12.1%)	31439 (50.4%)
4	2880011	52049	55.33	125 (0.2%)	19120 (36.7%)	6327 (12.2%)	26477 (50.9%)
5	2861803	49932	57.31	118 (0.2%)	18220 (36.5%)	5773 (11.6%)	25821 (51.7%)
6	2674951	38760	69.01	157 (0.4%)	14376 (37.1%)	4414 (11.4%)	19813 (51.1%)
7	2665280	49516	53.83	196 (0.4%)	15127 (30.6%)	7294 (14.7%)	26899 (54.3%)
8	2443572	54281	45.02	114 (0.2%)	21392 (39.4%)	5828 (10.7%)	26947 (49.6%)
9	2142475	45907	46.67	102 (0.2%)	19176 (41.8%)	5543 (12.1%)	21086 (45.9%)
10	1682575	40900	41.14	99 (0.2%)	17167 (42.0%)	5140 (12.6%)	18494 (45.2%)
11	1624292	34761	46.73	89 (0.3%)	13378 (38.5%)	3803 (10.9%)	17491 (50.3%)
12	1462624	31448	46.51	100 (0.3%)	11768 (37.4%)	3670 (11.7%)	15910 (50.6%)
13	1185774	28235	42.00	63 (0.2%)	10111 (35.8%)	3402 (12.1%)	14659 (51.9%)

Table S1. Z.tritici Markers Summary. The table presents the number (n) of markers per chromosome, along with chromosome length and SNP density. Columns "High," "Low," "Moderate," and "Modifier" indicate the number and percentage of variants classified under each impact category per chromosome.

P.impact	**Annotation**	**Observations**
modifier	upstream_gene_variant	265330 (39.87%)
low	synonymous_variant	238670 (35.87%)
moderate	missense_variant	79744 (11.98%)
modifier	downstream_gene_variant	35083 (5.27%)
modifier	intergenic_region	17894 (2.69%)
modifier	5_prime_UTR_variant	7995 (1.2%)
modifier	3_prime_UTR_variant	7960 (1.2%)
low	splice_region_variant&intron_variant	6028 (0.91%)
modifier	intron_variant	2070 (0.31%)
low	splice_region_variant&synonymous_variant	1142 (0.17%)

Table S2. Top 10 most frequent annotations in Z.tritici

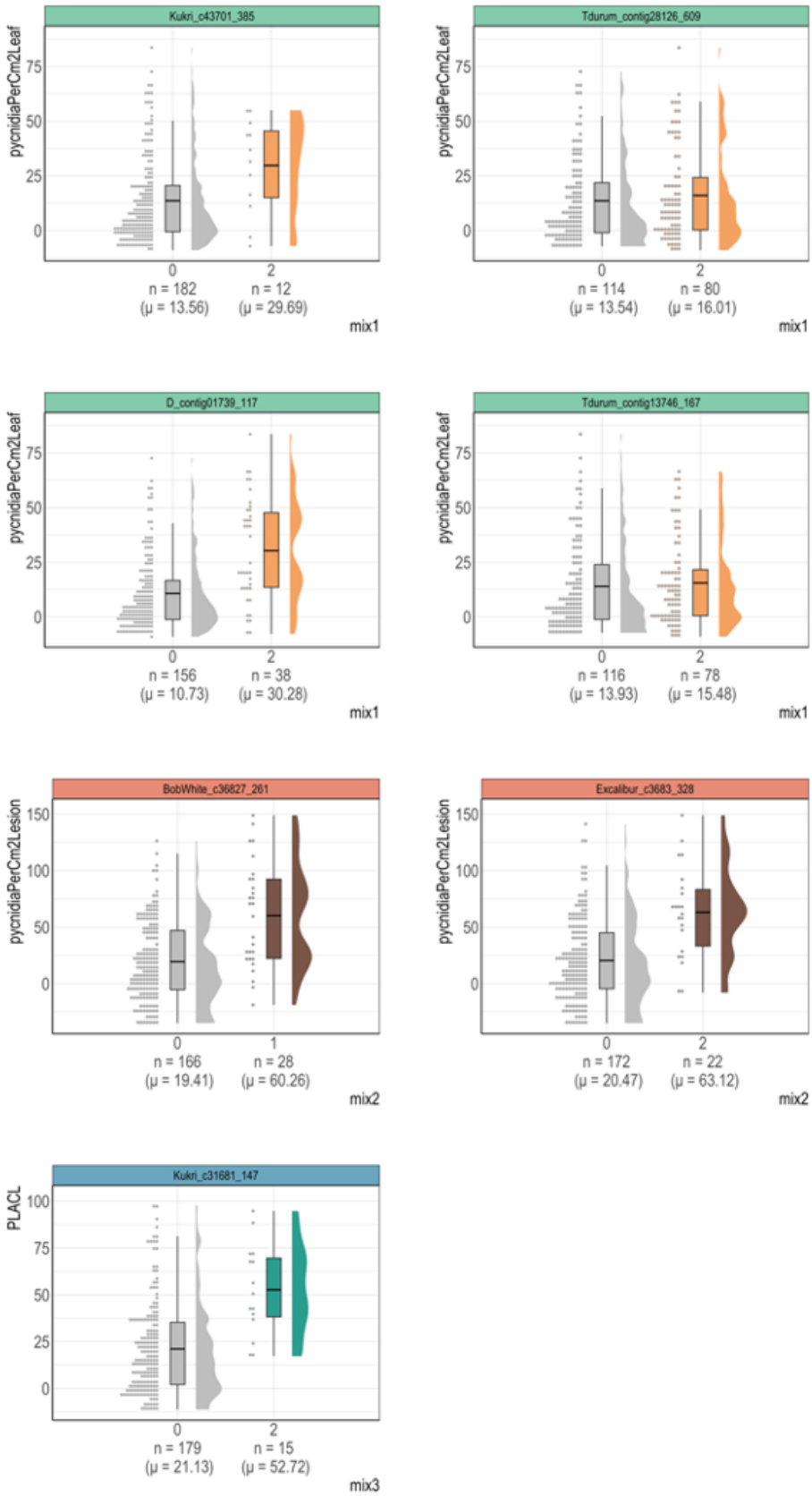

Fig. S5: **Allelic Distribution for Marker-Trait Associations in wheat GWAS**. Boxplots display the distribution of major (0) and minor (1) alleles for each significant marker-trait association. The header color indicates the mix treatment that triggered the association identified, while the boxplot color represents the associated trait.

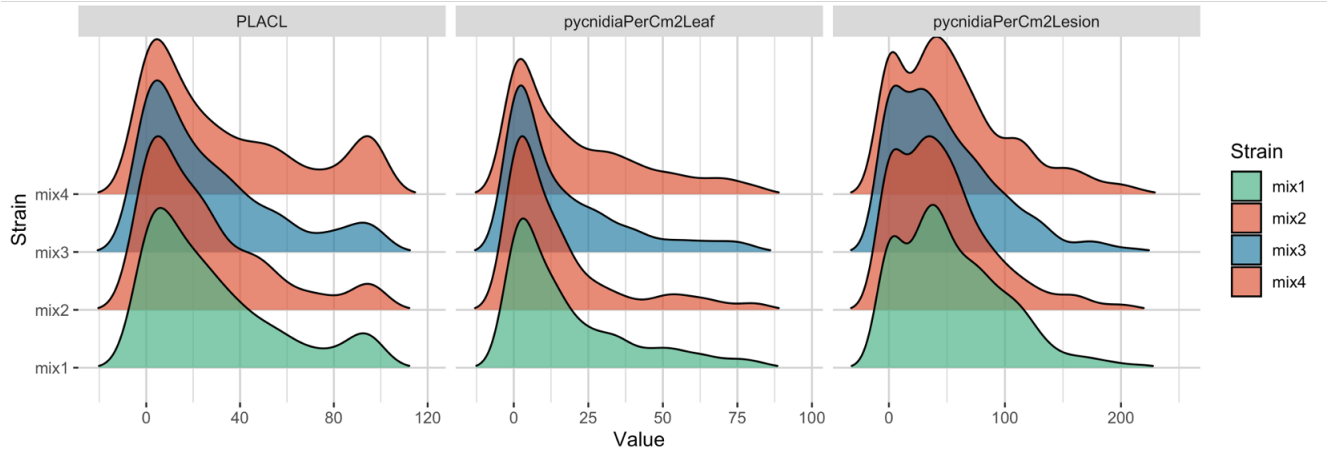

Fig. S6: **Density distribution of phenotypic values for each mix treatment**

Mix	SNP	Dist	Gene	Entry	Prot_name
Mix 1	Kukri_c43701_385	8.4	TraesCS1D02G176900	A0A3B5ZT27	Protein kinase domain-containing protein
				A0A9R1DMZ1	Uncharacterized protein
	Tdurum_contig28126_609	87.3	TraesCS2B02G195400	A0A3B6C549	RRM domain-containing protein
				A0A9R1EBW8	Uncharacterized protein
	D_contig01739_117	11.5	TraesCS2D02G372700	A0A3B6DGW9	TF-B3 domain-containing protein
				A0A9R1EW71	Uncharacterized protein
		12.0	TraesCS2D02G372800	A0A1D5UFU4	Glycosyltransferase (EC 2.4.1.-)
				A0A9R1EWI8	Uncharacterized protein
		39.9	TraesCS2D02G372900	A0A3B6DHI6	Zinc finger GRF-type domain-containing protein
				A0A9R1EWC1	Uncharacterized protein
	Tdurum_contig13746_167	503.1	TraesCS6B02G237700	A0A3B6PNJ2	AP2/ERF domain-containing protein
				A0A9R1IIC8	Uncharacterized protein
Mix 2	BobWhite_c36827_261	2.6	TraesCS1D02G185900	A0A3B5ZV49	DUF295 domain-containing protein
				A0A9R1DP17	Uncharacterized protein
		24.6	TraesCS1D02G186000	A0A3B5ZTC6	Uncharacterized protein
				A0A9R1DN24	Uncharacterized protein
		30.0	TraesCS1D02G186100	A0A3B5ZTD9	UBX domain-containing protein
				A0A9R1DN27	Uncharacterized protein
		36.5	TraesCS1D02G186200	A0A3B5ZV16	DUF4283 domain-containing protein
				A0A9R1IVY0	Uncharacterized protein
	Excalibur_c3683_328	447.9	TraesCS4A02G165100	A0A3B6HSG8	Adenylyl-sulfate kinase (EC 2.7.1.25)
				A0A3B6HW43	Adenylyl-sulfate kinase (EC 2.7.1.25)
				A0A9R1IK81	Uncharacterized protein
				A0A9R1LC25	Uncharacterized protein
Mix 3	Kukri_c31681_147	268.4	TraesCS1B02G168500	A0A3B5YVB4	Aldehyde oxygenase (deformylating) (EC 4.1.99.5)
				A0A9R1DC79	Uncharacterized protein

Table S3. Genes Associated with Marker-Trait Associations in Wheat. The table lists genes located within a 50 kb window upstream and downstream of each marker or the nearest gene when none were found within this range. Distances are measured in kilobases, and protein names were obtained from the UniProt database.

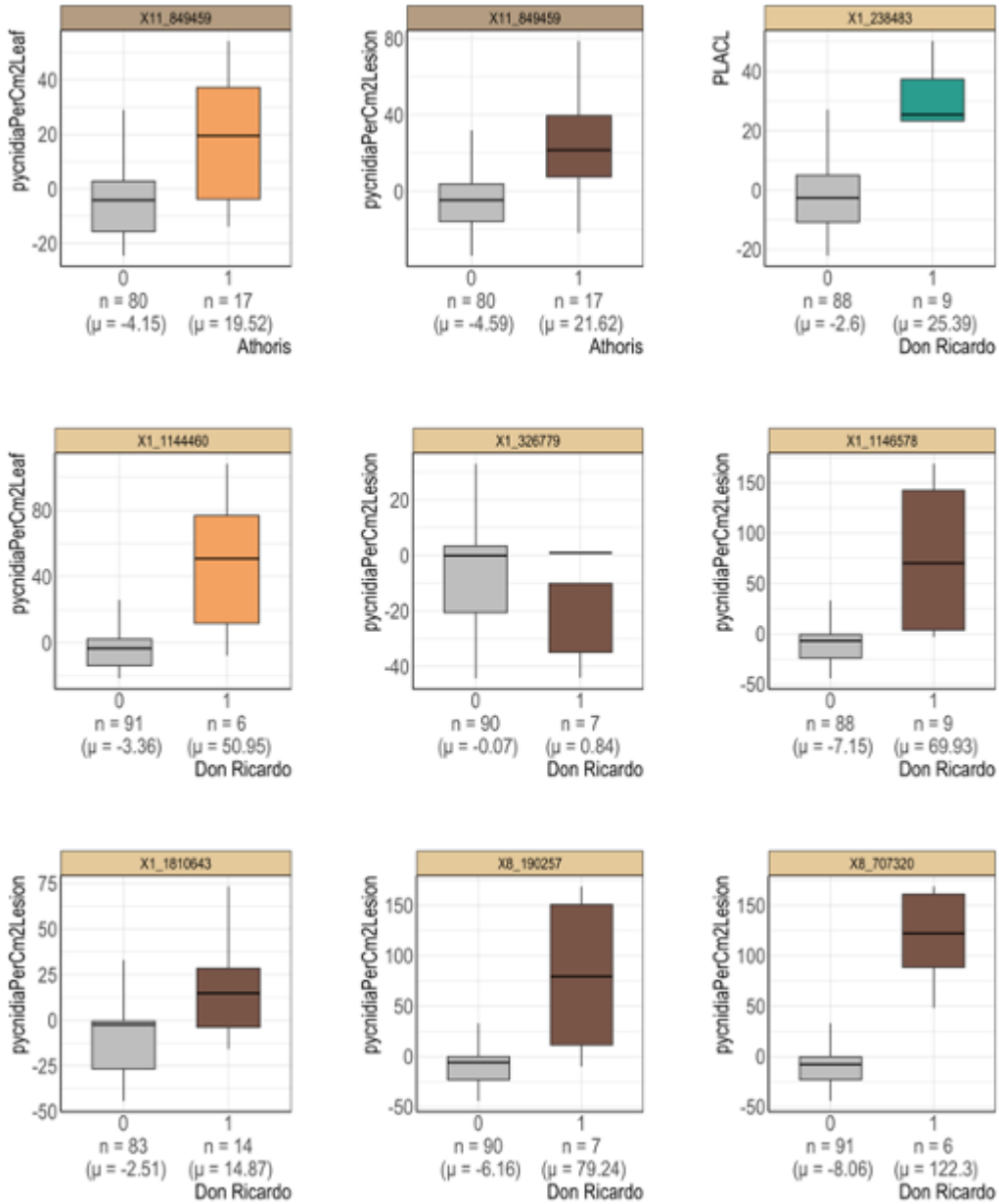

Fig. S7: **Allelic Distribution for Marker-Trait Associations in Fungal GWAS (I)**. Boxplots display the distribution of major (0) and minor (1) alleles for each significant marker-trait association. The header color indicates the cultivar where the association was identified, while the boxplot color represents the associated trait.

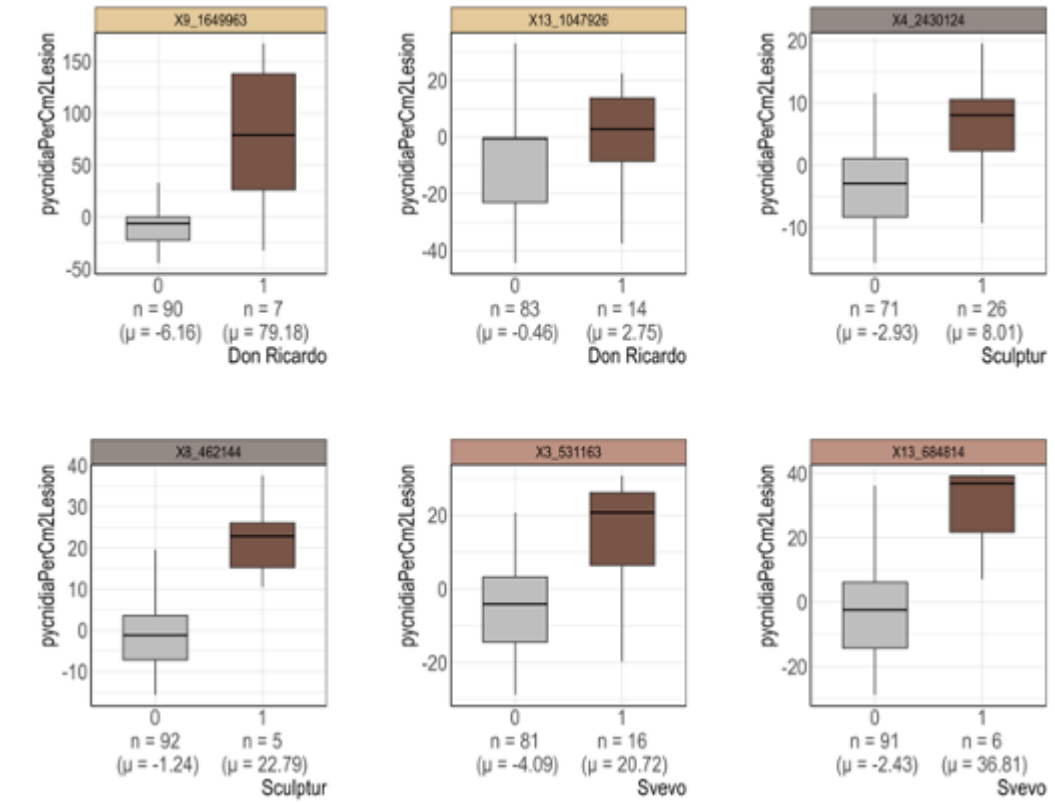

Fig. S8: **Allelic Distribution for Marker-Trait Associations in Fungal GWAS (II)**. Boxplots display the distribution of major (0) and minor (1) alleles for each significant marker-trait association. The header color indicates the cultivar where the association was identified, while the boxplot color represents the associated trait.

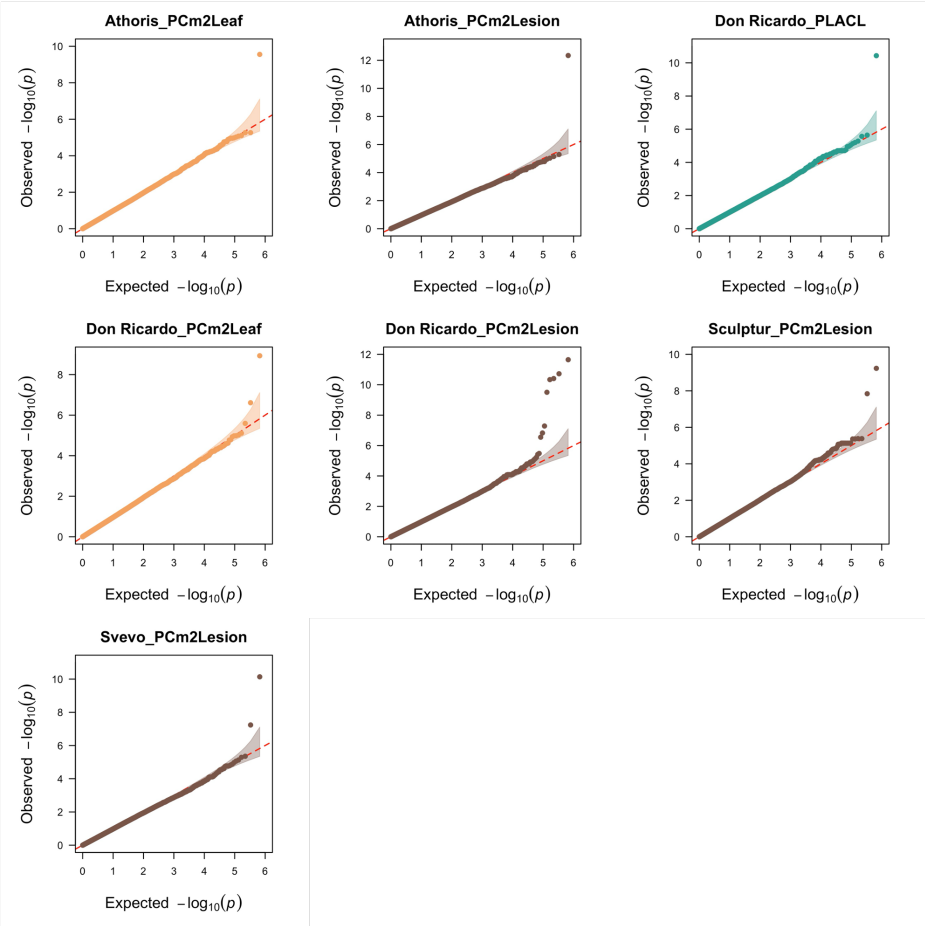

Fig. S9: Quantile-Quantile (QQ) plots corresponding to the traits in which significant hits were identified in the different cultivars.

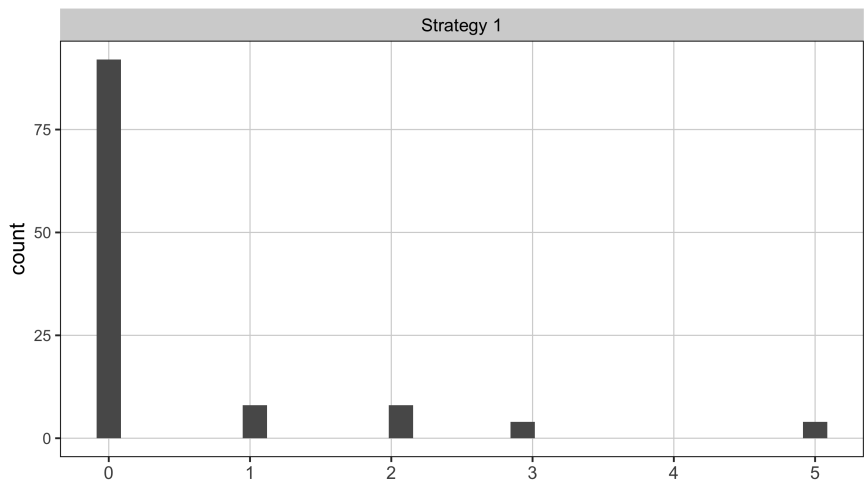

Fig. S10: **Histogram of GWAS Hits in Wheat-Mixes Cross-Validation**. The histogram shows the distribution of markers surpassing the Bonferroni threshold across 120 rounds of cross-validation (30 iterations × 4 covariance structures).

Cultivar	Traits	SNP	P-value	r^2	MAF	Distance	Gene
Athoris	PCm2Leaf	X11_849459	2.798187e-10	0.27	0.18	110	ZtIPO323_113470
	PCm2Lesion		4.558347e-13	0.26	0.18	110	ZtIPO323_113470
Don Ricardo	PCm2Leaf	X1_1144460	1.177673e-9	0.31	0.06	0	ZtIPO323_003820
			1.177673e-9	0.31	0.06	913	ZtIPO323_003810
	PCm2Lesion	X1_326779	1.488237e-7	0.00	0.07	816	ZtIPO323_000840
		X1_1146578	5.186265e-8	0.30	0.10	0	ZtIPO323_003820
			5.186265e-8	0.30	0.10	16	ZtIPO323_003830
		X1_1810643	3.12702e-10	0.02	0.14	0	ZtIPO323_006440
			3.12702e-10	0.02	0.14	1750	ZtIPO323_006450
			3.12702e-10	0.02	0.14	1536	ZtIPO323_006430
		X8_190257	4.59305e-11	0.30	0.07	0	ZtIPO323_088990
			4.59305e-11	0.30	0.07	0	ZtIPO323_089000
			4.59305e-11	0.30	0.07	472	ZtIPO323_088980
		X8_707320	3.906175e-11	0.61	0.06	1655	ZtIPO323_090540
		X9_1649963	1.893691e-11	0.30	0.07	1564	ZtIPO323_102580
			1.893691e-11	0.30	0.07	0	ZtIPO323_102590
			1.893691e-11	0.30	0.07	647	ZtIPO323_102600
		X13_1047926	2.251093e-12	0.00	0.14	5100	ZtIPO323_125710
	PLACL	X1_238483	3.699475e-11	0.28	0.09	0	ZtIPO323_000490
			3.699475e-11	0.28	0.09	712	ZtIPO323_000500
			3.699475e-11	0.28	0.09	1695	ZtIPO323_000480
Sculptur	PCm2Lesion	X4_2430124	5.846945e-10	0.26	0.27	0	ZtIPO323_059020
			5.846945e-10	0.26	0.27	1615	ZtIPO323_059010
			5.846945e-10	0.26	0.27	1771	ZtIPO323_059030
		X8_462144	1.441852e-8	0.27	0.07	0	ZtIPO323_089890
			1.441852e-8	0.27	0.07	0	ZtIPO323_089900
			1.441852e-8	0.27	0.07	1816	ZtIPO323_089910
Svevo	PCm2Lesion	X3_531163	5.787659e-8	0.22	0.16	0	ZtIPO323_039410
			5.787659e-8	0.22	0.16	1339	ZtIPO323_039400

Table S4. Genes Associated with Marker-Trait Associations in Z.tritici. The table lists genes located within a 2 kb window upstream and downstream of each marker or the nearest gene when none were found within this range. Distances are measured in base pairs (bp), and protein names were obtained from the latest annotation available (Lapalu et al., 2023)

Gene	Position	Description	Aa	Eff	SP	TM	IPR
ZtIPO323_000480	chr1:236211-236788	UPP	177	-	0	0	NA
ZtIPO323_000490	chr1:237794-238957	UCP MYCGRDRAFT_106743	258	Y	1	0	NA
ZtIPO323_000500	chr1:239195-240148	UCP MYCGRDRAFT_88622	318	-	0	0	NA
ZtIPO323_000840	chr1:323663-325963	Ca2+/calmodulin-dependent protein kinase	713	-	0	0	NEK Serine/Threonine Protein Kinase
ZtIPO323_003810	chr1:1141409-1143547	Aldehyde dehydrogenase (NAD+) like protein	480	-	0	0	Aldehyde dehydrogenase LUC3-l
ZtIPO323_003820	chr1:1143611-1146585	putative ABC transporter	834	-	0	2	ATP-binding cassette sub-family D
ZtIPO323_003820	chr1:1143611-1146585	putative ABC transporter	834	-	0	2	ATP-binding cassette sub-family D
ZtIPO323_003830	chr1:1146594-1148506	ferric reductase-like transmembrane component	568	-	0	7	Ferric/Cupric Reductase Transmembrane Component
ZtIPO323_006430	chr1:1804779-1809107	putative oxidoreductase	358	-	0	2	Short-chain dehydrogenase/reductase SDR
ZtIPO323_006440	chr1:1809298-1811836	CAT2 catalase	747	-	0	0	Catalase, mono-functional, haem-containing
ZtIPO323_006450	chr1:1812393-1814082	26S proteasome non-ATPase regulatory subunit 9	237	-	0	0	26S Proteasome non-ATPase regulatory subunit 9
ZtIPO323_113470	chr11:849569-853734	ochratoxin A non-ribosomal peptide synthetase	1038	-	0	0	Adenylate-forming Reductase
ZtIPO323_113470	chr11:849569-853734	ochratoxin A non-ribosomal peptide synthetase	1038	-	0	0	Adenylate-forming Reductase
ZtIPO323_124400	chr13:679175-687422	polyketide synthase	2627	-	0	0	Polyketide, Nonribosomal Peptide Biosynthesis Enzymes
ZtIPO323_125710	chr13:1053026-1056780	histidine kinase like protein	999	-	0	NA	Two-component histidine protein kinase
ZtIPO323_039400	chr3:527862-529824	Choline oxidase	543	-	0	0	Glucose-methanol-choline oxidoreductase
ZtIPO323_039410	chr3:530530-532485	Betaine aldehyde dehydrogenase	514	-	0	0	Aldehyde dehydrogenase
ZtIPO323_059010	chr4:2427396-2428509	benzoquinone reductase	206	-	0	0	Flavoprotein WrbA-like
ZtIPO323_059020	chr4:2429578-2431254	phthalate transporter like protein	479	-	0	12	Major facilitator superfamily
ZtIPO323_059030	chr4:2431895-2432434	uncharacterized protein MYCGRDRAFT_92832	180	-	0	0	NA
ZtIPO323_088980	chr8:187972-189785	glycosyltransferase family 32 protein	344	-	0.22	2	Glycosyltransferase domain-containing protein
ZtIPO323_089000	chr8:189780-192636	tRNA-guanine transglycosylase family protein	453	-	0	0	0
ZtIPO323_088990	chr8:189828-190891	Altered inheritance of mitochondria protein 6	315	-	1	0	Histone acetyltransferase RTT109-like
ZtIPO323_089890	chr8:459383-463143	uncharacterized protein MYCGRDRAFT_94965	494	-	0	0	Histone acetyltransferase RTT109-like (IPR051236)
ZtIPO323_089900	chr8:459956-463652	oligomeric golgi complex component	283	-	0	0	COG complex component, COG2
ZtIPO323_089910	chr8:463960-465126	mitochondrial 54S ribosomal protein MRPL1	311	-	0	0	Ribosomal protein uL1/ribosomal biogenesis protein
ZtIPO323_090540	chr8:708975-710975	Glutathione synthetase	513	-	0	0	Glutathione synthase
ZtIPO323_102580	chr9:1646494-1648399	unnamed protein product	376	-	0	0	NA
ZtIPO323_102590	chr9:1648629-1650432	unnamed protein product	448	-	0	0	NA
ZtIPO323_102600	chr9:1650610-1653327	putative transporter	512	-	0	12	Major facilitator superfamily

Table S5. Functional Annotation of Genes Identified in the Fungal GWAS. The table provides functional annotations for genes identified in the fungal GWAS. *Aa* represents protein length in amino acids, *Eff* indicates the probability of the protein being an apoplastic effector, *SP* denotes the presence of a signal peptide, *TM* specifies the number of transmembrane domains, and *IPR* refers to the InterPro family or domain associated with the protein.

Gene	4dpi	11dpi	13dpi	20dpi	Glu	log2FC_4dpi	log2FC_11dpi	log2FC_13dpi	log2FC_20dpi
ZtIPO323_000490	1.11	0.57	143.0	162.0	18.8	-4.08	-5.04	2.93	3.11
ZtIPO323_007800	4.03	601.0	256.0	13.1	18.4	-2.19	5.03	3.80	-0.498
ZtIPO323_060700	53.4	675.0	656.0	259.0	240.0	-2.17	1.49	1.45	0.114

Table S6. Expression Comparison of ZtIPO323_000490 and Known Z.tritici Effectors. Expression levels in planta at different days post-infection (dpi) are shown relative to the control medium Glucose (Glu), with values represented as log2 fold change (log2FC).